DESIGN GUIDELINES FOR IMPRESSED-CURRENT CATHODIC PROTECTION SYSTEMS ON SURFACE-EFFECT SHIPS

NAVAL SHIP RESEARCH AND DEVELOPMENT CENTER

MAY 1975

DISCLAIMER NOTICE

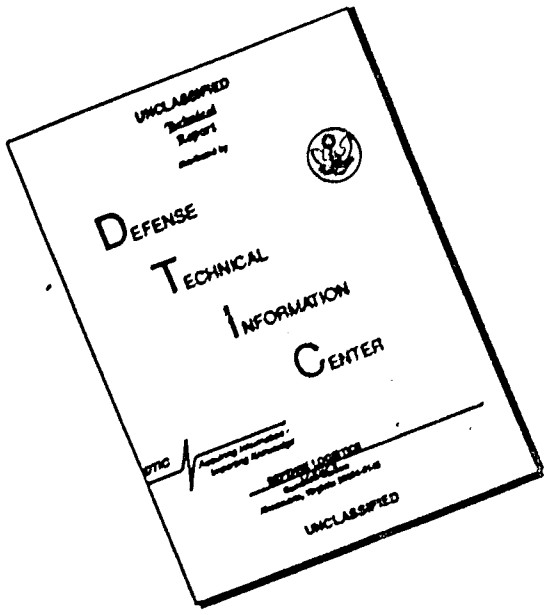

THIS DOCUMENT IS BEST QUALITY AVAILABLE. THE COPY FURNISHED TO DTIC CONTAINED A SIGNIFICANT NUMBER OF PAGES WHICH DO NOT REPRODUCE LEGIBLY.

Unclassified

SECURITY CLASSIFICATION OF THIS PAGE (When Data Entered)

REPORT DOCUMENTATION PAGE		READ INSTRUCTIONS BEFORE COMPLETING FORM
1. REPORT NUMBER 4531	2. GOVT ACCESSION NO.	3. RECIPIENT'S CATALOG NUMBER AD. A009 765
4. TITLE (and Subtitle) DESIGN GUIDELINES FOR IMPRESSED-CURRENT CATHODIC PROTECTION SYSTEMS ON SURFACE-EFFECT SHIPS		5. TYPE OF REPORT & PERIOD COVERED Research & Development 6. PERFORMING ORG. REPORT NUMBER
7. AUTHOR(s) Harvey P. Hack		8. CONTRACT OR GRANT NUMBER(s)
9. PERFORMING ORGANIZATION NAME AND ADDRESS Naval Ship Research & Development Center Annapolis, Maryland 21402		10. PROGRAM ELEMENT, PROJECT, TASK AREA & WORK UNIT NUMBERS Task Area S4629 Project S4629 Work Unit 2813-154
11. CONTROLLING OFFICE NAME AND ADDRESS Naval Ship Research & Development Center Bethesda, Maryland 20084		12. REPORT DATE May 1975 13. NUMBER OF PAGES 51
14. MONITORING AGENCY NAME & ADDRESS(if different from Controlling Office)		15. SECURITY CLASS. (of this report) Unclassified 15a. DECLASSIFICATION/DOWNGRADING SCHEDULE

16. DISTRIBUTION STATEMENT (of this Report)

Approved for public release; distribution unlimited.

17. DISTRIBUTION STATEMENT (of the abstract entered in Block 20, if different from Report)

18. SUPPLEMENTARY NOTES

19. KEY WORDS (Continue on reverse side if necessary and identify by block number)

20. ABSTRACT (Continue on reverse side if necessary and identify by block number)

This report presents results of various tests performed to establish design guidelines for the use of impressed-current cathodic protection systems on surface-effect ships. These results show that commercially available reference cells can be used in this application, and that dielectric shield materials, which can withstand the applied voltages, are available.

(Cont)

DD FORM 1 JAN 73 1473

Unclassified

SECURITY CLASSIFICATION OF THIS PAGE (When Data Entered)

20. ABSTRACT (Cont)

Size limits were set for dielectric shields on the SES-100B. A protection potential of -1150 millivolts was found to protect galvanic couples of surface-effect ship materials adequately at 90-knot velocities. Finally, updated design guidelines for impressed-current cathodic protection systems on surface-effect ships are presented.

(Author)

ADMINISTRATIVE INFORMATION

This report was prepared under Task Area S4629, Project S4629, Work Unit 2813-154. The investigation was sponsored by the Surface Effect Ship Project Office, NAVSEA (PMS 304) (formerly NAVMAT (PM 17)). It fulfills the requirement for an interim report stated in sections 4.3 and 5.2 of the Surface Effect Ship Project Office revised statement of work entitled "Impressed Current Cathodic Protection of SES," 17 July 1974.

ACKNOWLEDGMENT

The author wishes to acknowledge the work of Mr. Boyce Miller who assisted in test design and data analysis.

LIST OF ABBREVIATIONS

A - ampere

A/ft^2 - amperes per square foot

avg - average

° C - degrees Centigrade

dia - diameter

etc - and so forth

ft - feet

ft^2 - square feet

ft/s - feet per second

gpm - gallons per minute

g - gram

ICCP - impressed-current cathodic protection

ID - inside diameter

in. - inch

kn - knots

mA - milliampere

max - maximum

min - minimum

MPY - mils per year

mV - millivolt

No. - number

p/m - parts per million

psi - pounds per square inch

SES - surface-effect ship

V - volt

TABLE OF CONTENTS

TABLE OF CONTENTS (CONT)

The Naval Ship Research and Development Center is a U. S. Navy center for laboratory effort directed at achieving improved sea and air vehicles. It was formed in March 1967 by merging the David Taylor Model Basin at Carderock, Maryland with the Marine Engineering Laboratory at Annapolis, Maryland.

Naval Ship Research and Development Center
Bethesda, Md. 20034

MAJOR NSRDC ORGANIZATIONAL COMPONENTS

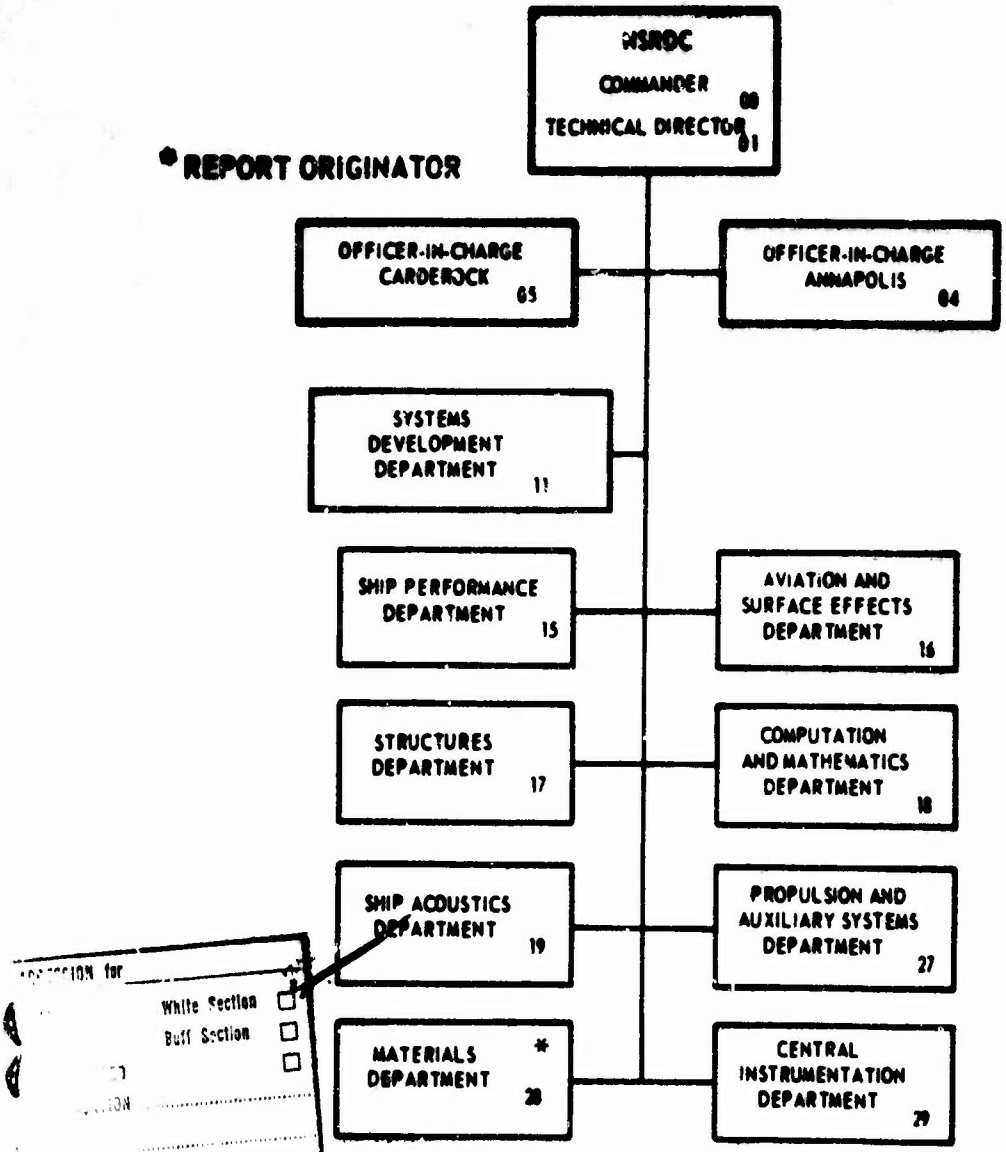

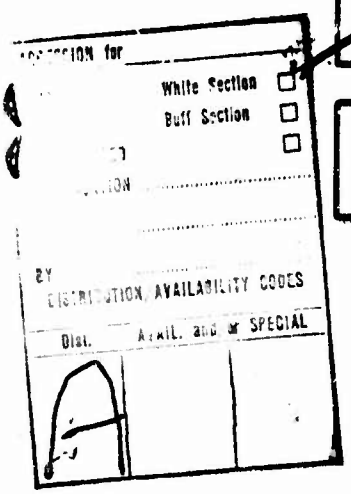

INTRODUCTION

Present day and future surface-effect ships are very weight-critical. Therefore, aluminum alloys, specifically 5083, 5086, and 5456 in the H-116 and H-117 tempers, are used in major structural applications, including external plating on the sidewalls. In contrast, auxiliary structures such as rudders, stabilizers, and propulsors frequently require materials with higher strengths than aluminum. Since aluminum alloys are anodic to all major structural metals in seawater, use of these high-strength materials will establish galvanic couples that will accelerate corrosion of the aluminum hull plating, with possible loss of watertight integrity.

To prevent this adverse galvanic action, cathodic protection should be employed. The action of a cathodic protection system is to polarize the cathodic materials (high-strength alloys) to the corrosion potential of the aluminum hull plating, thereby eliminating the driving force for the galvanic attack.

To this end, separate active (impressed-current) and passive (sacrificial anode) systems have previously been investigated. Studies of passive systems have indicated that they impose weight, drag, and maintenance penalties which are greater than those resulting from the active system. Although passive systems are generally used for cathodic protection and may possibly be used to supplement an active system, they were not investigated in this program.

This investigation has concentrated on establishing design parameters for an active, impressed-current cathodic protection system for surface-effect ships. No practical experience has been gained to date on such systems where aluminum hulls are subjected to high operating velocities. As a result, design data, particularly regarding current levels and means to avoid overprotection corrosion, and design procedures have been previously generated for the installation and operation of such a system on board these advanced ships.

This report presents results of additional laboratory tests related to the use of impressed-current cathodic protection systems on surface-effect ships. The data generated by these tests have been related to system design and operation. The purpose, procedure, and results of each test is presented as a unit in the section entitled "Laboratory Experiments." Following that section, a discussion integrating these test results into the design methodology developed in earlier programs is presented in an effort to publish the most up-to-date design procedures in a single document.

LABORATORY EXPERIMENTS

COMMERCIAL REFERENCE CELLS

The purpose of this experiment was to determine whether commercially available reference cell units considered for SES* applications would maintain electrical continuity between the internal silver/silver chloride (Ag/AgCl) material and the seawater outside of the cell at ship velocities of up to 90 knots. The possible source of discontinuity would be cavitation bubbles at the opening to the cell.

Two reference cells, illustrated in figure 1, were selected for test. Cell 1 is a surface-mounted streamlined type which meets the requirements of MIL-E-23919. Water access to the internal material is gained through thirteen 1/16-inch holes. Cell 2 is cylindrical and recess-mounted. Water access is gained through one end of the cell which is open and has six 1/4-inch holes.

Each cell was mounted in a Plexiglas apparatus, which restricted the water flow across the surface of the cell to achieve the desired velocity, and provided adequate visibility of the flow at the cell surface. Electrical potential difference was monitored between the commercial cell and a small Ag/AgCl reference electrode mounted in a tube where the water velocity was essentially zero but with a direct seawater path to the commercial electrode. Seawater for the test was provided by three centrifugal pumps rated at 500 gallons per minute.

Although air was usually trapped in several of the holes in cell 1, at no time were all of the holes so blocked. At least four holes had water inside them at all velocities. White areas, assumed to be air pockets where the seawater had "broken away" from the surface of the cell, occurred on the trailing edge of the cell at all velocities. This "breakaway" of the water flow which occurred on the flat cell face beyond the holes may be due to ventilation. It was least severe at the higher velocities, probably due to the higher pressures involved. No visual breakaway or cavitation phenomena was observed with cell 2 up to a velocity of 60 knots. A failure of the test unit precluded testing at higher velocities.

A chart giving the results of the potential measurements for both cells is presented as table 1. An erratic potential drift of 1 to 7 mV was present at all times with both cells. Drift of this magnitude is insignificant relative to total system performance. At first glance, the potential appears to shift more positive with increasing pressures and velocities. This shift is on the order of 90 mV and is more significant relative to the total

*A list of abbreviations used in this text appears on page i.

system. A closer examination of the data indicates, however, that the positive shift is a function of the time at high velocity rather than of pressure at velocity. This follows because these readings did not return to their original low value when the test was shut down. Although the magnitude of drift is lower on cell 2, this result is true for both cells. This potential shift may be due to the test procedure and not necessarily a cell stability problem. Therefore, it should not be considered a major problem on the craft on the basis of these results alone.

TABLE 1
COMMERCIAL REFERENCE CELL DATA

Time minutes	Pressure psi	Approximate Velocity knots	Potential Difference Between Commercial Cell and Zero Velocity Cell, mV
		Reference Cell 1	
10	25	30	-8 to -14
11	50	40	1 to 5
		RESTART	
0	21	30	10 to 14
3	21	30	13 to 15
19	21	30	8 to 10
15	21	30	7 to 9
		RESTART	
0	39	30	25 to 26
5	39	30	30 to 31
6	122	60	40 to 42
10	122	60	45 to 50
		RESTART	
0	75	50	40 to 42
1	120	60	56 to 57
5	120	60	66 to 68
10	150	90	81 to 88
15	150	90	87 to 91
16	0	0	75 to 80
17	0	0	80 to 85
		Reference Cell 2	
0	25	25	-17 to -20
1	50	30	6 to 7
3	49	30	12 to 15
4	120	60	33 to 34
		SHUTDOWN	

Reference cell 1 is not recommended for SES applications due to the possibility of cavitation damage to the ship from its use. Reference cell 2 appears to be suitable for SES applications, but it may be advisable to shield the cell from the high velocity water flow by means of a porous plug inserted in front of the cell, flush with the outer hull. This would eliminate the problem of drift, if indeed it would have existed in the final system. This plug would establish a seawater path from the cell to the outer hull and would eliminate the possibility of cavitation generated by the hole through which the cell would ordinarily "see" the hull potentials.

OVERPROTECTION

As the potential of aluminum is shifted more electronegative, a point is reached where hydroxide ions are generated, creating a high pH at the specimen surface. Since aluminum experiences rapid chemical attack in such basic solutions, the potential must be maintained more positive than the limit of overprotection corrosion. The purpose of these studies was to determine the electrical potential below which aluminum experiences intense degradation due to overprotection corrosion.

To determine the limit of overprotection at high velocity, experiments were run on 1- x 4-inch aluminum specimens in the high velocity test apparatus at a nominal velocity of 80 knots (actual velocity, 82 knots) for 7 days. Specimens were held at -1200 to -1750 mV, relative to Ag/AgCl, in 50-mV increments. This range was selected to bracket the known limit of overprotection at zero velocity of -1500 millivolts. Table 2 presents the results of these experiments.

TABLE 2
RESULTS OF OVERPROTECTION EXPERIMENTS

Potential mV	Weight Loss, g	Corrosion Rate, MPY	Specimen Appearance
-1200	.350	52.4	No visible corrosion
-1250	.320	47.8	No visible corrosion
-1300	.270	40.3	No visible corrosion
-1350	.326	48.8	No visible corrosion
-1400	.306	45.7	No visible corrosion
-1450	.236	35.8	No visible corrosion
-1500	.289	43.2	Light corrosion, leading edge
-1550	.301	44.9	Light corrosion, leading edge
-1600	.328	49.1	Light corrosion first 1/2 inch of specimen
-1650	.315	47.1	Light corrosion first 1/2 inch of specimen
-1700	.309	46.2	Light corrosion first 1/2 inch of specimen
-1750	1.874	280.1	Severe general corrosion

The data indicate that severe overprotection corrosion occurred on aluminum specimens at 80 knots at potentials more electronegative than -1700 millivolts. Therefore, these potentials should be avoided on aluminum hulls of SES operating at 80 knots, as there is a possibility of overprotection corrosion occurring under these circumstances. Earlier tests for the Advanced Hydrofoil System Office have shown that aluminum specimens will suffer degradation due to overprotection in still water (<2 ft/s) at potentials more electronegative than -1500 millivolts. Unless the ICCP system output varies with craft velocity, overprotection may occur if the potential anywhere on the hull is between -1500 and -1700 mV when the craft operates below 80 knots. Hull potential should therefore never be more electronegative than -1500 mV, unless the system output is designed to vary with craft velocity.

FLAME-SPRAYED ALUMINUM COATINGS

The purpose of this study was to determine the feasibility of using a flame-sprayed aluminum coating on the noble metal appendages of the SES in order to minimize galvanic effects.

Specimens of 17-4PH stainless steel, Inconel 625, and titanium 6Al-4V were prepared for high velocity testing and flame sprayed with 10 mils of aluminum. These specimens, along with a solid aluminum control specimen, were tested at seawater velocities of about 70 knots for 30 days. Seawater used was drawn directly from Wrightsville Sound, North Carolina, and was unfiltered. Open-circuit potentials were monitored to determine the extent of coating degradation, and the specimens were examined at the end of the test.

Figure 2 is a presentation of the results of this experiment. The data are presented as deviations in corrosion potential from the solid aluminum control specimen. Coatings on all of the materials generally began to deteriorate by the end of the second day as indicated by the potential shifts. The coating was significantly deteriorated on the 17-4PH and Inconel specimens by the fourth day, whereas, major deterioration on the titanium specimens did not occur until the eighth day. Coatings on the 17-4PH and Inconel specimens were essentially nonexistent by the eighth day, however, the titanium specimens did not reach this state until the fifteenth day.

The above test is rather severe because silt assumed to be present in the water, may give rise to abnormally high removal rates due to abrasion. Other coating procedures, including the use of fillers or intermediate materials to improve adhesion, may result in aluminum coatings which will survive at SES velocities.

Although the use of flame-sprayed aluminum coatings on SES appendages is not presently recommended, further study using different coating procedures and test methods may give more favorable coating life.

PIPE STUDIES

The purpose of these studies was to determine the amount of current needed to polarize the inside surface of a water-jet nozzle, or any through-hull duct, near the point of water exit, to the protective potential of the hull, and to determine how far into the nozzle the current would travel. This knowledge is needed to determine the demands of a water-jet propulsion system on current output of the impressed-current cathodic protection system.

Four different materials were tested: 304 stainless steel, titanium 6Al-4V, 70/30 copper-nickel, and Monel. Eight-foot pipes of each material were obtained with nominal inside diameters of 4, 2, and 1 inch (the smallest Monel pipe was 3/4-inch ID). These pipes were sealed at one end and coated on the exterior surface. Salt bridges and Ag/AgCl reference cells were located at 1-foot intervals down the length of the pipe, with the closest cell 1 inch from the opening. The pipes were then immersed in seawater and current was delivered to the inside surface from a platinized titanium anode. The test setup is illustrated in the upper portion of figure 3. The voltage of the number 1 reference cell was adjusted stepwise to the following protection potential values: -950, -1050, -1100, -1150, and -1200 millivolts, and the corresponding current was noted. At each voltage level the potential of each reference cell was recorded 2 or 3 times at 30-minute intervals so that an accurate picture could be obtained of the potential profile down the length of the pipe interior.

To establish the effect of water velocity, the experiment was repeated with the 3/4- and 1-inch pipes with water flowing at 90 knots through the pipe towards a specially designed anode at the end, as illustrated in the lower part of figure 3. Only one set of readings was taken at each current level.

Figure 4 summarizes the effect of velocity on the potential curves at -1150 mV for 1-inch pipes of all four materials. The greater the initial drop-off of the potential curve, the more current is necessary to polarize the material. For example, the initial drop-off of the stainless steel at zero velocity is twice as great as the titanium; therefore, the corresponding current for stainless steel is greater than for titanium (12.6 compared to 9.9). Tests at higher velocities invariably have a greater initial drop-off and, therefore, require greater currents than the same pipes at zero velocity. For example, for 1-inch titanium pipe, the drop-off at 90 knots is twice that at 0 knots, and the current at 90 knots is, therefore, greater than at 0 knots (29 compared to 10). Most of the curves began to rise slightly near the far end of the pipe. This effect was reproducible in these tests, but the exact cause could not be determined. Table 3 indicates that the current at 90 knots is 3 times greater than at zero velocity for the stainless steel and titanium alloy, and 12 times greater for 70/30 copper-nickel. The behavior of Monel was anomalous due to an initially high current at low velocity which decayed rapidly. Also, it can be

seen that the currents for all materials, except Monel, at 0 knots vary linearly with pipe diameter or exposed area.

TABLE 3
MAXIMUM CURRENT WHEN CELL 1 POTENTIAL WAS -1150 MV

Diameter in.	Velocity knots	304 Stainless Steel, mA	Titanium mA	70/30 Cu-Ni mA	Monel mA
1	90	37.4	29.4	450	430[1]
1	0	12.9	10.0	38.5	323[1,2]
2	0	27.8	33.4	100	74.1
4	0	76.4	68.5	164	210

[1] 3/4 inch.
[2] A later test where the potential was held at a constant -1150 mV required a similar high current initially which decayed by more than an order of magnitude over the 60-minute test period.

Figure 5 summarizes the effect of internal pipe diameter on the current distribution. Except for small pipes of titanium and Monel, there is good agreement of the potential data when plotted versus distance divided by the pipe diameter, instead of versus distance directly. The curves for 1-inch titanium and, to a much lesser extent, for 3/4-inch Monel do not exactly correspond to the curves of the larger pipes. The reason for these two deviations is unknown, but there is sufficient agreement among the rest of the data to support the conclusion that the "throwing power," or effective protection distance down the inside of a pipe, of an impressed-current cathodic protection system is a direct function of the internal pipe diameter. Table 3 indicates that the amount of current necessary to polarize the internal surface of the end of a pipe to -1150 mV increases 2 to 3 times as the pipe diameter doubles. This is true for all materials tested except the anomalous 3/4-inch Monel pipe.

Figure 6 summarizes the effec of different materials on the internal potential profile of the pipes. The curves are the same as in figure 5 but are superimposed for comparison. The two nickel- and copper-containing alloys behaved similarly, having the most rapid initial potential drop-off, with a sharp change to constant potential at about 30 pipe diameters. Stainless steel, although having an initial drop-off almost as steep as the nickel-copper alloys, does not level off as abruptly at 30 diameters and continues to drop until about 60 diameters. Titanium, like the nickel- and copper-containing alloys, experiences a sharp change to constant potential at 30 diameters, but the initial drop-off is not as great.

These curves indicate that the Monel and copper-nickel alloy are less easily polarized than the other materials tested and therefore should require greater currents. Looking at table 3, it can be seen that 70/30 copper-nickel does indeed require about 3 times the protection current at 0 knot than the stainless steel or titanium alloy. Again, the behavior of the Monel pipe is anomalous, but currents to this pipe are higher than to the stainless steel or titanium.

Figure 7 illustrates the effect of the deviation of protection potential from -1150 mV on the internal potential profiles of the pipes. The vertical axes of the curves are the differences, at the location specified, between the pipe potentials when the protection levels are -1150 mV, and when they deviate from -1150 mV by 50, -50, -100, and -200 millivolts. These plots are therefore the deviation from the profiles at the -1150 mV protection level. In all cases, the deviation is high near the anode, indicating a large change in internal potential with protection potential, and decreases as distance from the anode increases. Larger pipes tended to have greater deviations farther from the anode than smaller pipes. The 304 stainless steel and the Monel pipes had larger deviations down the length than the other alloys. The potential profile of these materials far from the anode is therefore more dependent on protection level than is that for the other alloys. These curves may be useful to determine the degree of protection if dissimilar metals are used in a water-jet propulsion system.

Table 4 presents current data for the pipes at various protection potential levels. Generally, the maximum current increased with more electronegative potentials. The exception to this, 304 stainless steel, exhibited currents which decayed with time at a slower rate at more negative potentials, ultimately reaching higher values at more electronegative potentials. Current needed to protect titanium pipe increased 1 1/2 to 3 times as the protection potential was lowered from -950 to -1200 millivolts. All of the 70/30 Cu-Ni and Monel pipes, with the exception of the 3/4 inch Monel pipe, experienced current increases at -1200 mV of 3 1/2 to 5 times the value at -950 millivolts.

The effect of potential within a ±50-mV range from -1150 mV on the protection current of all pipes except the 3/4-inch Monel was relatively minor. This indicates that a 50-mV change in the control potential of an impressed-current cathodic protection system will make little difference in the current demanded from that unit to polarize a water-jet nozzle to the protection potential. The small Monel pipe, although experiencing unusually high maximum currents at the more electronegative control potentials, also exhibited a rapid decay of these currents with time. There is presently no explanation for why this phenomenon was observed on the 3/4-inch pipe and not on the larger sizes.

TABLE 4
MAXIMUM CURRENTS AT VARIOUS PROTECTION LEVELS, MA

Protection Potential, mV	1-Inch Pipe	2-Inch Pipe	4-Inch Pipe
	304 Stainless Steel		
-1200	14.9	30.7	97.5
-1150	12.9	27.8	76.4
-1100	12.5	27.1	76.3
-1050	11.7	27.5	79.5
-950	13.5	32.4	98.2
	Titanium		
-1200	10.7	36.7	74.5
-1150	10.0	33.4	68.5
-1100	9.5	29.5	56.9
-1050	7.8	28.5	56.5
-950	3.7	22.6	48.1
	70/30 Cu-Ni		
-1200	92.2	260.0	308.0
-1150	38.5	100.1	164.0
-1100	23.4	70.8	125.0
-1050	26.0	61.2	108.1
-950	23.7	48.0	88.0
	Monel		
-1200	388.0(1)	128.4	360.0
-1150	323.0(1)	74.1	210.0
-1100	59.0(1)	55.6	153.0
-1050	27.0(1)	46.0	116.0
-950	15.7(1)	36.5	92.5

(1) 3/4 inch - A later test where the potential was held at a constant -1150 mV required an initially high current which decayed by more than an order of magnitude over the 60-minute test period.

Due to the small amount of current reaching the pipe ends, longer pipes should not require significantly more total current than the 8-foot sections. Therefore, the maximum currents required for water-jet nozzles of any size can be assumed to be the same as for the 8-foot sections, and these values can be used for system design. Table 5 is such a list of design currents. The figures at 90 knots for 2- and 4-inch-diameter nozzles were extrapolated from the 1-inch-pipe data. The maximum current, occurring in a 4-inch 70/30 Cu-Ni nozzle at 90 knots, is less than 2 amperes, which should be negligible compared to the total output of an ICCP system. As previously explained, this current is not expected to change significantly at control potentials of -1100 to -1200 millivolts.

TABLE 5
WATER-JET NOZZLE DESIGN CURRENT REQUIREMENTS
AT -1150 MILLIVOLTS, AMPERES

Nozzle, ID, in.	0 Knot	90 Knots
304 Stainless Steel		
1	0.013	0.038
2	0.028	0.082
4	0.077	0.225
Titanium		
1	0.010	0.030
2	0.034	0.102
4	0.069	0.207
70/30 Cu-Ni		
1	0.039	0.450
2	0.100	1.154
4	0.164	1.893
Monel		
1	0.323	0.430
2	0.075	0.100
4	0.210	0.280

SPECIMEN SIZE STUDIES

In previous experiments using small aluminum specimens, the corrosion potential was found to vary greatly with time. The purpose of this experiment was to determine whether the open-circuit potential variations experienced by small specimens are a localized surface phenomenon which would therefore be of lower magnitude on larger specimens due to an averaging effect. If this is not the case, then the fluctuations are probably due to changes in certain seawater variables which might be determinable.

Two specimens of 5456 aluminum, 1 x 4 x 1/4 inch and 18 x 24 x 1/4 inch, were exposed in natural seawater for 33 days, cleaned, and reexposed in a seawater trough at a velocity of 2 ft/s for an additional 31 days. Open-circuit potentials of the specimens were monitored and the results are shown in figure 8. Since the magnitude of potential drift was essentially the same for both specimen sizes, the drift could not be caused by localized surface phenomena which would average out on larger specimens. In addition, the potentials of the two specimens drifted in the same direction at the same time, indicating that both were controlled by the same variable. This variable was assumed to be a seawater chemistry parameter.

To test this hypothesis, the small specimen was exposed at 2 ft/s for an additional 7 days. The following were monitored twice daily: open-circuit potential, seawater temperature, salinity, pH, and dissolved oxygen content. The results are graphed in figure 9. There appears to be no definitive systematic effect of any of the seawater variables on the open-circuit potential of the aluminum specimen. It is still possible that some other seawater variable not monitored, such as heavy-metal ion concentration, is the cause of the open-circuit potential drift experienced by aluminum in seawater.

This study shows that the range of corrosion potentials experienced by a surface-effect ship hull is likely to be as great as the range experienced in previous tests by the small test specimens (400-500 millivolts).

GALVANIC COUPLES

The purpose of this experiment was to check the applicability of the results obtained in previous high velocity laboratory tests to the protection of actual galvanic couples at high velocity.

A high velocity apparatus which consisted of a nozzle connected to two pumps rated at 500 gpm each was used for these tests. Unfiltered seawater from Wrightsville Sound, North Carolina, was used. Modifications were made to house galvanic couples in the nozzle, as shown in figure 10. Specimen sizes were identical in dimensions to the standard high velocity specimens, but half the length. A noble metal specimen was placed in the upstream half of the normal specimen position and an aluminum specimen was placed downstream, separated by a 1/16-inch nonmetallic spacer. Electrical connection was made to the specimens through similar metal contact screws. The wiring diagram is also illustrated in figure 10. Tests were conducted on uncoupled control specimens, unprotected couples, and protected couples.

Test duration was 2 weeks, and the nominal velocity was 80 knots. Readings were taken daily. Readings taken were: potentials of uncoupled control specimens, potentials of unprotected couples, galvanic current for all couples, and protection current for the protected couples. The corrosion rate of each specimen was determined using weight loss data.

Results of the experiments are shown in table 6. Positive protection and galvanic currents are defined by the arrows in figure 10. Protection current is always in the same direction (cathodic). A positive galvanic current indicates protection; a negative current indicates galvanic corrosion. The corrosion rates in the table do not behave as expected; i.e., the rate of coupled aluminum is not higher than for uncoupled or protected aluminum. The primary mode of material removal in this test may be abrasion by silt. If this is the case, the abrasion may mask the galvanic corrosion effects.

TABLE 6
RESULTS OF HIGH VELOCITY GALVANIC COUPLE EXPERIMENTS

	17-4PH and Aluminum			Titanium and Aluminum		
	Min	Avg	Max	Min	Avg	Max
Potentials, mV						
Uncoupled						
Noble	-158	-104	-59	-188	-81	-26
Al	-951	-908	-870	-963	-923	-872
Unprotected couple	-728	-688	-609	-860	-812	-780
Galvanic current, mA						
No protection	-3.30	-4.52	-5.10	-0.80	-2.19	-2.60
-1025 mV	3.60	6.44	8.90	2.62	7.27	12.00
-1100 mV	11.00	17.91	21.50	8.60	14.92	19.00
-1150 mV	6.40	17.27	21.60	10.80	20.14	23.60
Protection current, mA						
-1025 mV	32.7	65.2	95.0	6.0	21.2	31.0
-1100 mV	45.5	104.7	125.0	11.0	40.0	51.6
-1150 mV	43.0	108.3	135.0	34.0	61.5	72.9
Corrosion rate, mils/year						
Open circuit						
Noble		0.2			0.2	
Al		103			98	
Coupled						
Noble		0.3			0.4	
Al		98			105	
-1025 mV						
Noble		0.1			0.4	
Al		102			103	
-1100 mV						
Noble		0.1			0.4	
Al		85			94	
-1150 mV						
Noble		0.2			0.4	
Al		89			93	

Although the corrosion rate data in table 6 are suspect, current data should still be valid. A comparison of predicted protection current values, calculated by multiplying previously generated current densities by the specimen area, and observed values is presented in table 7. The actual current maximums never exceed the predicted maximums, supporting the maximum current density predictions. Frequently, however, the observed minimum current was below the predicted minimum. This would suggest that the minimum current densities at 90 knots, which were used in the calculations, are inaccurate and should be revised. The new minimum current densities, calculated by dividing the actual minimum current by the specimen area, are as follows: 17-4PH at -1025 and at -1100 mV, 1.28 and 1.78 A/ft^2; and titanium at -1025 and at -1100 mV, 0.23 and 0.40 A/ft^2.

Due to the difficulty in predicting minimum current demands on the cathodic protection system from the laboratory tests, the use of power supplies which have a minimum current rating of zero amperes is recommended.

TABLE 7
COMPARISON OF PREDICTED AND OBSERVED CURRENTS

Couple, mV	Predicted Ranges					Observed Total Protection Current, mA		
	Current Density, A/ft²		Current on 0.0256 ft² Specimens, mA		Total Protection Current, mA			
	Noble	Al	Noble	Al		Min	Avg	Max
17-4PH								
-1025	3.34-6.75	0-0.29	85.5-172.9	0-7.4	85.5-180.3	32.7	65.2	85.0
-1100	3.18-5.97	0-0.23	81.4-152.9	0-5.9	81.4-158.8	45.5	104.7	125.0
Titanium								
-1025	1.18-3.72	0-0.29	30.4-95.3	0-7.4	30.5-102.7	6.0	21.2	31.0
-1100	0.40-1.83	0-0.23	10.2-46.9	0-5.9	10.2-52.8	11.0	40.0	51.6

ANODE PROFILES

The purpose of this study was to determine the potential profile around a hull-mounted anode. Once this profile is known, the dielectric shield size and shape can be selected to cover all areas around the anode which might be more electronegative than the critical potential where overprotection corrosion begins to occur.

Part I

Part I of this study was designed to determine the profile around a 4-foot anode mounted in an "infinite" hull to establish the profile shape and prove the test method before the more elaborate part II was performed.

For this purpose, a raft was constructed which could float on a body of seawater and have an anode and various potential measuring devices suspended in the seawater 1 to 2 inches below it. The raft, illustrated in figure 11, consisted of six sections of 1/4-inch plywood, backed by 3 inches of closed-cell foam and held together by wooden brackets and 2- x 4-inch lumber. In the center, fully immersed, was a 5- x 48-inch simulated anode made from 14 lengths of platinized titanium wire. Provisions were made to allow easy escape of any gases generated at the anode. Around the perimeter in a roughly circular configuration 32 feet in diameter, were two lengths of platinized titanium wire, supported by eight pieces of 2- x 4-inch lumber backed with foam. This wire was fully immersed and was used to simulate an infinitely distant cathode in the system.

Current was delivered from a set of lead-cadmium batteries in a nearby fiber glass work boat, through a resistance network and a length of AWG-00 welding cable, to the anode. The current delivered by the anode to the cathode was fed through the welding cable back to the batteries, and measured by means of a 100-ampere, 0.0005-ohm shunt.

The potential field generated by this current flow through the seawater was measured by an array of 48 silver/silver chloride reference cells spaced at 6-inch intervals in various patterns, shown in figure 12, in one quadrant of the raft. The other three quadrants were assumed to be symmetrical to the one measured. Leads from the reference cells were fed through a switching box to a high-impedance digital voltmeter located in the work boat. Their potentials were compared to a remote silver/silver chloride reference cell suspended in the seawater next to the work boat outside of the potential field between the anode and cathode; see figure 11. This cell was used as a standard because it was located in a similar position to the controlling cell of a working ICCP system.

Tests were conducted in natural seawater which had a depth of about 12 to 15 feet at a sheltered area near Wrightsville Beach, North Carolina. Sets of potential readings were taken at current levels of 10.7, 18.1, 50.1, 62.4, 76.4, 95.1, and 121.5 amperes. Results of these measurements are presented in table 8. It was later discovered that cells 20 and 39 had broken off before the test, but the silver lead wire, which had some silver chloride on it from the cell manufacturing process, appeared to generate satisfactory readings without the main body of the cell attached.

Two representative potential profiles are presented in figures 13 and 14. Figure 13 represents the maximum potentials at any given distance. These occur on a line perpendicular to the anode located midway along its length (cells 1-11). Figure 14 represents the potentials along a line perpendicular to the anode located at one end (cells 12-22). The potential values decay rapidly near the anode and more slowly at larger distances from the anode. As the current is increased, the potentials near the anode rise in about the same proportion as those farther away, giving rise to a sharper gradient at the anode at higher currents than at lower currents. Potentials at any set distance from the anode ends are invariably lower than those at the same distance on the line perpendicularly bisecting the anode.

Data at two current levels, 50 and 120 amperes, are presented as equipotential lines in figures 15 and 16. These lines were calculated by interpolation of the data. The potential pattern appears to be elliptical with the higher current level in figure 16 having a greater line density, or potential gradient, near the center than the lower current level in figure 15.

TABLE 8

REFERENCE CELL READINGS, VOLTS VERSUS Ag/AgCl

Reference Cell No.	Anode Current, amperes							
	0	10.7	18.1	50.1	62.4	76.4	94.1	121.5
1	0.002	1.200	2.200	6.08	7.55	9.20	11.25	14.60
2	0.006	0.800	1.420	3.90	4.80	6.90	7.18	9.30
3	0.007	0.550	1.000	2.75	3.40	4.20	5.10	6.60
4	0.006	0.420	0.780	2.15	2.65	3.25	4.00	5.20
5	0.007	0.340	0.610	1.70	2.10	2.60	3.15	4.00
6	0.005	0.270	0.510	1.40	1.75	2.15	2.60	3.40
7	0.007	0.230	0.425	1.18	1.46	1.80	2.20	2.90
8	0.006	0.200	0.360	1.01	1.25	1.55	1.90	2.40
9	0.005	0.140	0.270	0.75	0.93	1.15	1.40	1.80
10	0.004	0.105	0.200	0.56	0.70	0.87	1.05	1.30
11	0.004	0.085	0.160	0.44	0.545	0.69	0.85	1.10
12	0.004	1.080	2.060	5.75	7.18	8.70	10.70	13.90
13	0.007	0.555	1.035	2.85	3.57	4.30	5.35	6.95
14	0.007	0.400	0.760	2.10	2.62	3.20	4.00	5.15
15	0.009	0.325	0.605	1.70	2.10	2.60	3.20	4.15
16	0.007	0.275	0.520	1.40	1.79	2.10	2.70	3.50
17	0.010	0.230	0.430	1.20	1.50	1.84	2.28	2.95
18	0.006	0.195	0.370	1.00	1.28	1.57	1.93	2.50
19	0.008	0.170	0.320	0.89	1.11	1.38	1.69	2.19
20	0.025	0.110	0.200	0.64	0.82	1.03	1.25	1.60
21	0.004	0.095	0.175	0.52	0.65	0.80	1.00	1.30
22	0.005	0.080	0.140	0.40	0.515	0.64	0.79	1.00
23	0.004	1.360	2.560	7.10	8.82	10.60	13.10	17.00
24	0.007	0.550	1.040	2.90	3.60	4.40	5.40	7.00
25	0.007	0.360	0.670	1.85	2.32	2.78	3.47	4.50
26	0.008	0.280	0.520	1.49	1.87	2.18	2.72	3.50
27	0.007	0.220	0.420	1.12	1.37	1.74	2.17	2.80
28	0.007	0.185	0.350	0.96	1.19	1.45	1.80	2.35
29	0.006	0.155	0.295	0.82	1.03	1.25	1.55	2.02
30	0.007	0.115	0.215	0.60	0.76	0.92	1.15	1.50
31	0.006	0.090	0.170	0.47	0.58	0.71	0.90	1.17
32	0.003	0.065	0.130	0.355	0.45	0.57	0.68	0.90
33	0.006	0.425	0.800	2.20	2.73	3.28	4.10	5.30
34	0.024	0.250	0.495	1.10	1.52	1.79	2.30	2.80
35	0.005	0.210	0.395	1.10	1.39	1.68	2.10	2.70
36	0.005	0.170	0.315	0.88	1.10	1.32	1.67	2.15
37	0.006	0.135	0.235	0.70	0.90	1.08	1.34	1.74
38	0.005	0.110	0.205	0.58	0.73	0.88	1.10	1.45
39	0.006	0.090	0.160	0.48	0.60	0.73	0.92	1.20
40	0.005	0.070	0.140	0.395	0.50	0.61	0.79	1.00
41	0.009	0.180	0.340	0.94	1.20	1.43	1.78	2.30
42	0.004	0.170	0.315	0.88	1.10	1.32	1.66	2.17
43	0.005	0.150	0.285	0.795	1.00	1.20	1.50	1.96
44	0.007	0.135	0.255	0.72	0.90	1.10	1.37	1.78
45	0.006	0.155	0.290	0.80	1.01	1.22	1.53	1.99
46	0.004	0.170	0.275	0.80	1.08	1.27	1.63	2.05
47	0.009	0.125	0.250	0.71	0.90	1.10	1.37	1.80
48	0.006	0.124	0.240	0.66	0.84	1.02	1.27	1.65

In summary, the potential pattern from a 5-inch by 4-foot anode delivering current to an infinitely distant cathode is an ellipse, with the highest potential at a given distance from the anode located along the line bisecting the anode. Within experimental error, the potentials increase in proportion to the currents, the effect being the same at any distance.

Part II

The purpose of part II of this study was to further define the potential profile around a hull-mounted anode, specifically, on the SES-100B surface-effect ship. To determine the distortion in the field due to the unique hull shape and proximity of noble metal appendages to the anode in this ship, a second raft was constructed.

This was a full-scale, plywood, watertight mock-up of the below-waterline area of a 22-foot-long section of one sidewall of the surface-effect ship operating under conditions where maximum current is expected from the protection system (15-inch depth, 60 knots), as shown in figure 17. The raft itself is shown in figure 18, and the wiring diagram is shown in figure 19. Next to the stabilizer on the bottom surface was mounted a commercially available 4-foot strip anode. This is the suggested location for the anode on the craft. Current from this anode was delivered through the seawater to coils of platinized titanium wire at locations simulating the noble metal rudder, stabilizer, propeller and gearbox assembly, and the aluminum hull areas forward of the dielectric shield. Current was supplied to the anode from twelve 2-volt lead-cadmium storage batteries connected in series, through a set of dropping resistors and a current measuring network consisting of meters and shunt resistors. Heavy AWG-00 welding cable was employed wherever high currents were expected, to minimize voltage losses. Current levels to the various coils were determined by calculating the actual current required by each appendage. This calculation, which is based on wetted surface areas and maximum current densities, is detailed in figures 20 and 21.

Measurement of the potential field around the anode was accomplished by the use of 48 silver/silver chloride reference cells located in a network on the external surface of the raft, as shown in figure 22. Leads from the reference cells were connected through a switching box to a high-impedance digital voltmeter which compared their potentials to a remote silver/silver chloride reference cell suspended in the seawater far from the raft. Cell 31 was disconnected from the surface of the raft during transportation, and its exact position during the test is unknown.

Tests were conducted in natural seawater which had a depth of 8 to 12 feet at a sheltered area near Wrightsville Beach, North Carolina. Two sets of readings were taken. The first set, shown in figure 20, simulated the effect of a partially isolated propeller system (scaled to 1/2 of total output due to battery limitations), and the second set, shown in figure 21, simulated the effect of a completely isolated propeller.

Potential profiles of the two situations appear as figures 23 and 24. These potentials are plotted as a function of distance from the anode in various directions. Since these potential curves will be used only for determining potential differences between two locations, the absolute magnitude of the potentials is irrelevant. Therefore, in order to simplify the analysis, the curves have been shifted so that the protection potential is located at a point 10 feet forward of the anode near where the impressed-current system controlling reference cell will be located; 7 feet aft of the anode, since this is the limit of the aluminum hull in this direction; and 1 1/2 feet up the inside of the sidewall and 3 1/2 feet along the bottom and up the outside of the sidewall at the waterline.

In figure 23, the curves aft of the anode both have a steep gradient, as expected from the high current flow in this direction. The curves forward of the anode show a steep gradient near the anode which tapers off as distance from the anode increases. Close to the hull end of the raft, the gradient begins to increase again as the current concentrates at the cathode. On the real craft this would not take place, since the current is distributed over a large area, and the curves would approximately follow the dashed lines.

The overprotection limit is marked at -1.5 volts. Wherever the hull potential is more electronegative than this value, overprotection will occur on areas of the hull not covered by dielectric shield material. Therefore, the dielectric shield must be applied to any area where the potential curve exceeds the overprotection line. A practical limit to the size of the dielectric shield can therefore be determined from the curves.

To consider the case of an electrically isolated propeller (this assumption would be reasonable whenever the propellers were rotating), figure 23 should be consulted. Looking forward of the anode, it can be seen that the shield size must extend about 6 feet forward of the anode, to the point where the curve crosses the overprotection line. To determine the shield size aft of the anode, the potential curves aft of the anode are consulted. The gradient is so steep aft of the anode that the shield must extend to within a foot of the gearbox housing (located 7 feet aft of the anode). It is therefore convenient to increase the size of the shield to cover the hull all the way back to this housing, thus adding a safety factor.

Figure 24 should be used to determine the athwartships symmetry of the shield. Looking outboard of the anode (left side), the dielectric shield distance can be seen to be slightly less than 3 feet. In the other direction, the stabilizer appears to have absorbed most of the current and the curves never rise to the level where a dielectric shield is necessary. Since these curves were taken at an assumed on-cushion draft of 15 inches, it is logical that they would show little shield needed above the anode. At higher drafts, more current will be delivered up the sidewalls so that the shield distances in this direction should be a few feet greater than indicated by this study.

The final dielectric shield should therefore extend from the gearbox to a point 6 feet in front of the anode and about 3 feet up the sidewalls on both the inboard and outboard sides.

DIELECTRIC SHIELD MATERIALS

The purpose of this study was to evaluate the resistance of various dielectric shield materials to high anode voltages. No other tests were performed on these materials. Two aluminum specimens, 4 inches square, were coated with a rubberized dielectric shield material, and two specimens about 1 foot square were coated with an epoxy mastic material. All panels were affixed in test racks which allowed only the coated faces to come in contact with the seawater, and one panel of each material had the coating pierced with a pinhole-sized drill to simulate a coating flaw. The racks were immersed in natural seawater, and the panels held at -1? volts relative to platinized titanium anodes mounted nearby. Total test time was 316 days for the epoxy mastic and 212 days for the rubberized coating.

Results of the exposures indicate that both materials performed well under these conditions, with no evidence of blistering or peeling. The rubberized coating was superior to the epoxy mastic, however, allowing no overprotection of the aluminum to occur except at the pinhole. Corrosion products at this location sealed the hole to prevent further damage. The epoxy mastic was more brittle and exhibited very small failures at the edge of the test rack. The pinhole in the coating allowed more material removal to take place before it was sealed by corrosion products.

Both materials would probably perform adequately at the anode potentials necessary for cathodic protection of surface-effect ships. Tests should be conducted to determine their resistance to high seawater velocities, however. The epoxy mastic is easy to apply by troweling. The rubberized coating would probably withstand accidental impact damage better due to its inherent flexibility. In addition, the rubberized coating presents a smoother finish, creating less hydrodynamic drag or turbulence than the epoxy mastic, unless the latter is applied with great care.

DESIGN GUIDELINES

The design procedure for an impressed-current cathodic protection system for a surface-effect ship is as follows:

- Determination of maximum current required.
- Selection of power supply and controller.
- Determination of number, size, type, and location of anodes.
- Determination of type and configuration of dielectric shields.
- Determination of location of reference cells.
- Alteration of craft design to ease interface with system.

DETERMINATION OF MAXIMUM CURRENT REQUIRED

The optimum control potential to minimize the galvanic effects of the appendage materials on the aluminum hull plating is in the vicinity of -1150 millivolts. At this potential, galvanic corrosion will be completely suppressed almost all of the time and minimized the rest of the time. The exact control potential may be changed slightly from this value depending on experience gained by operating systems on other surface-effect ships. The effects of this potential on other materials in the ship should be considered. For instance, 17-4PH steel when heat treated to higher strength levels experiences hydrogen embrittlement when coupled to aluminum. When protection is applied at a potential more electronegative than the mixed potential of the aluminum/17-4PH couple, this effect may be intensified.

The effective area of each material must next be calculated at all operational modes. This can be done as follows:

- The draft of the craft at various velocities and in various operational modes must be determined.
- The wetted area of each part made of the material, as determined from craft blueprints and the draft at the specific operational mode, must be multiplied by the expected percentage of coating defects on that part to obtain the effective area of that part. Uncoated parts will have a defect fraction of 100%; whereas, the defect fraction for coated parts must be estimated from the expected coating degradation rates and expected maintenance schedules. The maximum fraction of damaged coating must be used as the defect fraction and will usually not exceed 10%. The area of propellers and shafting must not be included, unless the propellers are not rotating in the operational mode being

considered (dockside). The internal areas of water-jet nozzles must not be included in these area calculations, since the current to them will be calculated and added at a later time.

- The sum of the effective areas of each part made of the material being considered is the effective area of that material.

The maximum current required at each operational mode must now be calculated by multiplying the area of each material by the maximum current density for that material at the expected operating speeds at that draft. This current density can be found in table 9.

TABLE 9
DESIGN MAXIMUM CURRENT DENSITIES FOR CONTROL POTENTIAL OF -1150 MILLIVOLTS

Velocity knots	Design Current Density, A/ft^2
5456 Aluminum	
0	-
28	0.58
55	1.19
77	0.23
17-4PH Stainless Steel	
0	0.14
28	4.91
55	5.73
77	5.97
Ti-6Al-4V	
0	0.09
28	3.04
55	4.85
77	1.83
Inconel 625	
0	0.27
28	1.99
55	7.00
77	4.69

Values obtained for each material should be summed, and currents to water-jet nozzles added. This calculation can be summarized as follows:

$$I_{x,y} = A_{1,x} \times P_{1,y} + A_{2,x} \times P_{2,y} + \ldots + I_n N ,$$

where

$I_{x,y}$ = current at draft x, speed y.

$A_{1,x}$ = effective area of material 1 at draft x.

$A_{2,x}$ = effective area of material 2 at draft x.

$P_{1,y}$ = current density of material 1 at speed y (from table 9).

$P_{2,y}$ = current density of material 2 at speed y (from table 9).

N = number of wetted water-jet nozzles, intakes, etc.

I_n = currents required for water-jet nozzles, intakes, and any through-hull piping (from table 5).

This calculation should be performed for all expected operational modes, including dockside, cushionborne at low velocities, and cushionborne at high velocities. The maximum total current should then be the highest value calculated for the maximum current at any particular operational mode.

SELECTION OF POWER SUPPLY AND CONTROLLER

The selected power supply must be capable of converting ship's power into usable power for the anode. It must have the capacity to supply the maximum current calculated for any operational mode over long periods of time, with a current limiting device to prevent it from exceeding this value. It must also be able to limit its output to zero. A properly designed saturable reactor supply with a low-current bypass can be designed to meet these requirements. In addition, this unit offers the advantages of durability, resistance to transients, and intrinsic filtering.

The controller unit must be capable of controlling power supply output over its full range, with appropriate sensitivity to avoid slow reaction or overcompensation. A sensitivity adjustment and overload protection are desirable. Another necessary feature for any controller unit is fail-safe design, which will cause the controller output to reduce to zero in the case of system malfunction, such as open-circuited or shorted anode or reference cell wires, or excessive potentials at the edge of the dielectric shield.

Both units must have appropriate shielding and filtering to prevent them from picking up interference and broadcasting it to the anodes. Other considerations in the selection of these two units include physical size and weight relative to ultimate

location in the craft, ease of monitoring system function, reliability, overhaul requirements, stability, and ability to withstand marine atmospheres, vibration, and shock.

DETERMINATION OF NUMBER, SIZE, TYPE, AND LOCATION OF ANODES

Placement of anodes is critical in the design of an impressed-current system. Generally, anodes must be more concentrated in the vicinity of dissimilar metal appendages, since these will absorb a large portion of the anode current. They must be totally submerged under maximum velocity cushionborne operation to maximize their current-delivering capability. Other than this, anode placement and shape should be chosen to distribute the anode current evenly over the wetted surface areas. Consideration should also be given to remote mounting of the anodes far from the hull, such as at a point halfway between the sidewalls. Remote anode mounting would eliminate the need for dielectric shields which are the weakest link in the impressed-current system, and would permit more even distribution of the anode current.

Due to the high-speed of surface-effect ships, the anodes must be flush-mounted or faired into the hull. Flush-mounting is preferred but more difficult to achieve. A special SES design will have to be used. On surface-effect ships, limited submerged areas in the cushionborne mode place special requirements and limitations on the size, shape, and type of anodes needed. For example, the small on-cushion draft of a 100-ton SES necessitates the use of long, thin anodes in order to maintain continuous submersion.

DETERMINATION OF TYPE AND CONFIGURATION OF DIELECTRIC SHIELDS

Dielectric shields are used only if remote anode mounting is not employed. The best dielectric shield materials to date for use with hull-mounted anodes are a rubberized coating and a troweled-on epoxy mastic. The rubberized coating is hydrodynamically smooth, not as susceptible to damage, and contains an antifoulant. The epoxy mastic is easier to apply over irregular surfaces, and greater experience has been gained with its use.

Design of the shield is as critical as selection of the material of which it is constructed. The shield is applied to the hull around the anode for a specified minimum distance which is dependent on maximum anode current. If noble metals are located near the anode, the shield must be slightly extended in their direction, since the presence of these materials will tend to distort the potential profile around the anode due to the large amount of current these materials require. Coated appendages will distort the field less than uncoated appendages. Minimum dielectric shield radii for a 4-foot-strip anode, operating at about 50 amperes at a location next to the stabilizer on the SES 100B, are 3 feet up the sidewalls and 6 feet from the end.

The best available conservative values for the shield radius at higher anode currents, assuming no appendages are nearby, were established for conventional craft and are 7 feet for a 100-ampere anode and 11 feet for a 200-ampere anode. These radii are determined so that the hull potential never is more negative than -1.5 volts at the edge of the shield.

DETERMINATION OF LOCATION OF REFERENCE CELLS

The fully recessed reference cell mentioned in the laboratory tests is well suited for surface-effect ship use. It should be equipped with a porous plug to improve streamlining, and shielded cable should be employed so that stray electrical signals are not picked up and transmitted through the controller to the anodes.

Although a single reference cell is used to control the normal operation of the impressed-current system, usually at least two are installed. The second is used as a spare and to check the stability of the controlling reference cell. The reliability of these cells is important. On aluminum-hulled craft with properly designed and applied dielectric shields, reference cell failure may lead only to wasteful current excesses, but on craft with shield deficiencies, reference cell malfunction may increase the degree of overprotection corrosion experienced. Placement of the reference cells is also critical. Generally, they should be mounted well away from the anodes but not in areas that are completely sheltered from the anode current, for example, near corners or in areas near significant amounts of dissimilar metals, such as propellers. The general intent is to place the reference cells in an area well representative of overall hull potential. Additional cells may be mounted in areas of concern, for instance, near appendages, provided that they are not used to control the normal operation of the system but are for information and safety only. One such reference cell should be placed at the edge of the dielectric shield. This cell could act as a safety device to provide the controller with information concerning when overprotection conditions are reached at the shield edge, so that the anode current can be reduced accordingly.

ALTERATION OF CRAFT DESIGN TO EASE INTERFACE WITH SYSTEM

The ship design must be altered to accommodate the system components and locations selected. Structural design modifications to the hull may have to be performed in order to accommodate hull-mounted equipment. Space for hull-mounted and on-board equipment may be restricted, but adequate access space must still be provided, as the equipment must be monitored. Anode cable lengths should be kept to a minimum, and, where possible, should not be run through fuel or ballast tanks or near instruments that are sensitive to strong magnetic fields. Power generating facilities must be compatible with the system. Hull-mounted equipment may cause drag which will affect ship performance. In short, all

aspects of the system must be considered before final equipment selection and installation.

RECOMMENDED ADDITIONAL RESEARCH

- Remote Anode Studies - Conduct a feasibility study, and develop a working design for a remote anode system to be used on SES. Use of such an anode would eliminate the dielectric shield and associated problems and provide a more uniform distribution of anode current.

- Effect of Silt on SES Materials - Conduct experiments to determine whether the presence of silt in the seawater used for high-velocity tests will lead to high current densities and material removal rates due to abrasion.

- Effect of Protection Potentials on Titanium and 17-4PH Stainless Steel - Conduct experiments to determine if the highly electronegative potentials associated with a cathodic protection system will induce adverse effects such as hydrogen embrittlement on the titanium and 17-4PH stainless steel SES appendages.

- Effect of Seawater Temperature of Protection Current Densities - Conduct systematic experiments to determine the effect of seawater temperature on the protection current density of SES materials.

- Current Densities at -1.15 Volts - Conduct experiments to establish the current densities needed to polarize SES materials to -1.15 volts.

- Hull Anode Design - Design a streamlined hull-mounted anode for SES use which will have minimum drag and cavitation characteristics combined with high current capabilities and long life.

- Controller and Power Supply Design - Design a controller and power supply which are compatible with SES. Both units should operate from craft power, 28 volts, 400 hertz. The controller should have provisions for current suppression if the reference cell at the shield edge exceeds -1.5 volts, and should be fail-safe. The power supply should be of the saturable-reactor type with maximum current limiting circuitry and current bypass circuitry to allow reduction of output to zero amperes.

- Coating Degradation - Determine the expected rate of hull coating degradation at SES velocities, and determine the effect of the control potential on this coating degradation rate. This data can be used to obtain a defect area fraction.

- Velocity Effects on Dielectric Shield Materials - Determine the effects of high velocities on the candidate dielectric shield materials. Determine the optimum shield edge configuration to minimize the possibility of shield damage.

- Pilot System - Install a pilot impressed-current cathodic protection system onboard a 100-ton SES, preferably the SES-100B, in order to verify the design methodology and current data, and to gain operational experience on such a system before installation on the 2000-ton SES.

Cell 1

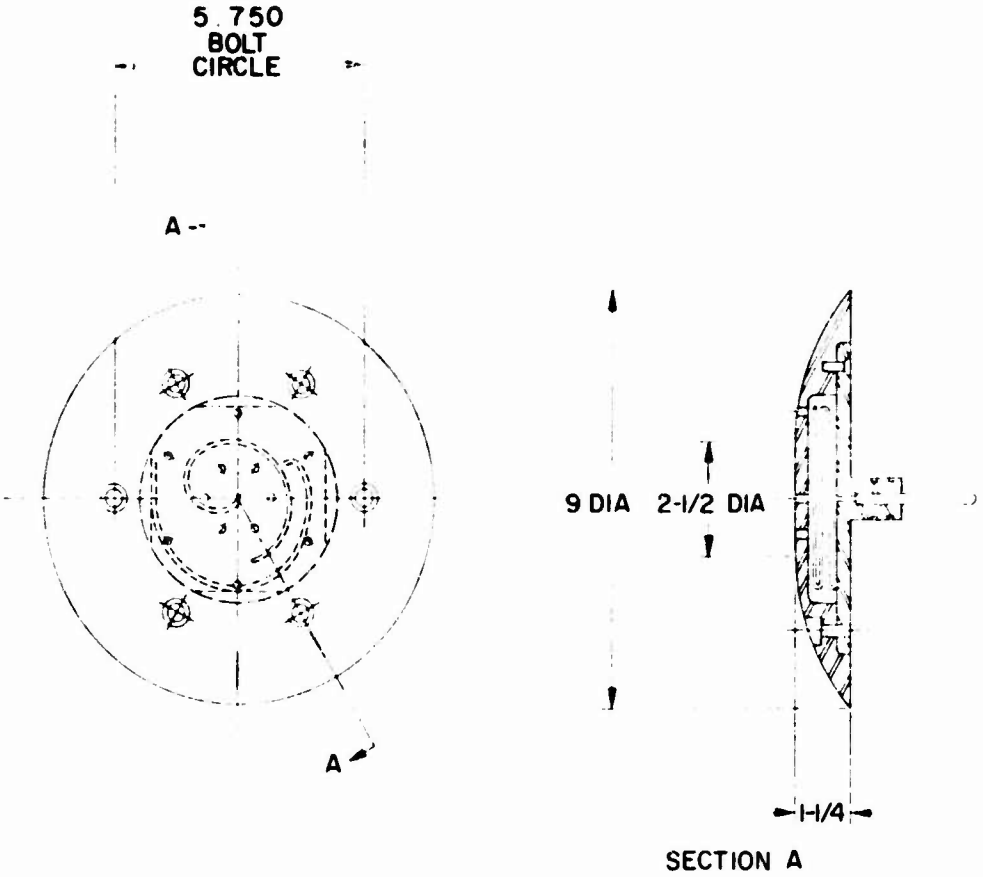

Cell 2

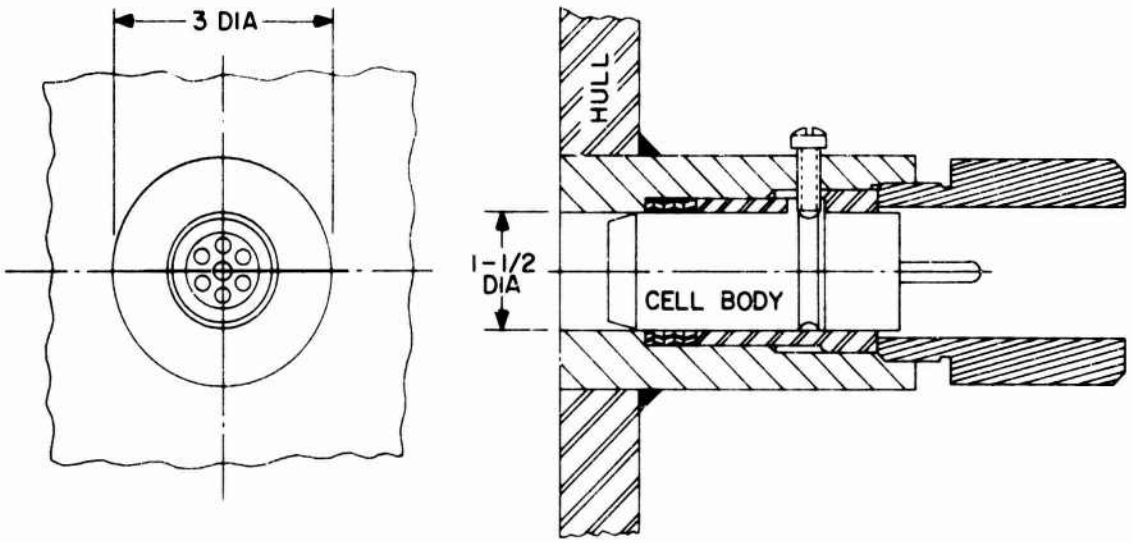

Note: All dimensions in inches.

Figure 1
Commercial Reference Cells

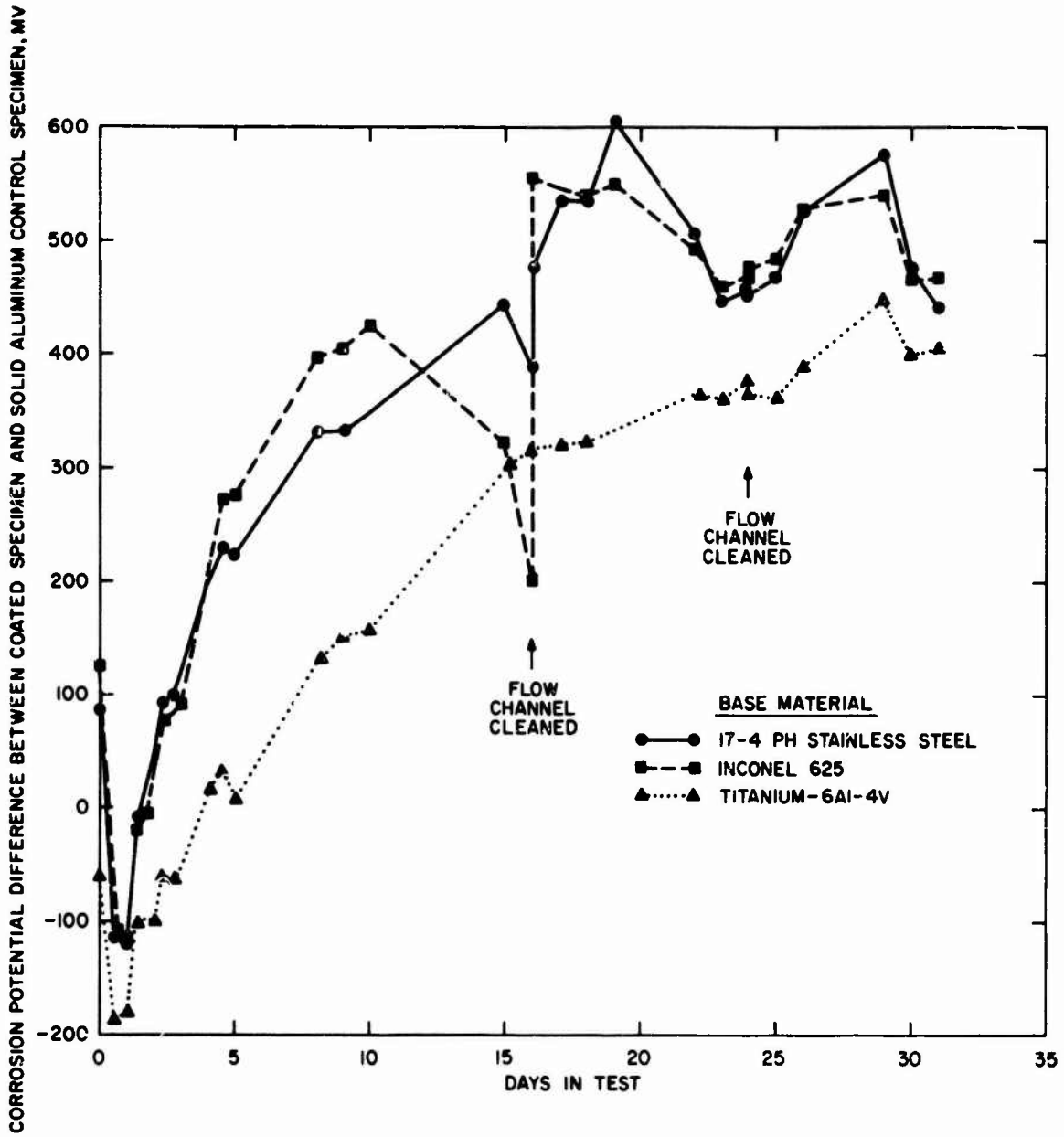

Figure 2
Results of Flame-Sprayed Coatings Experiments

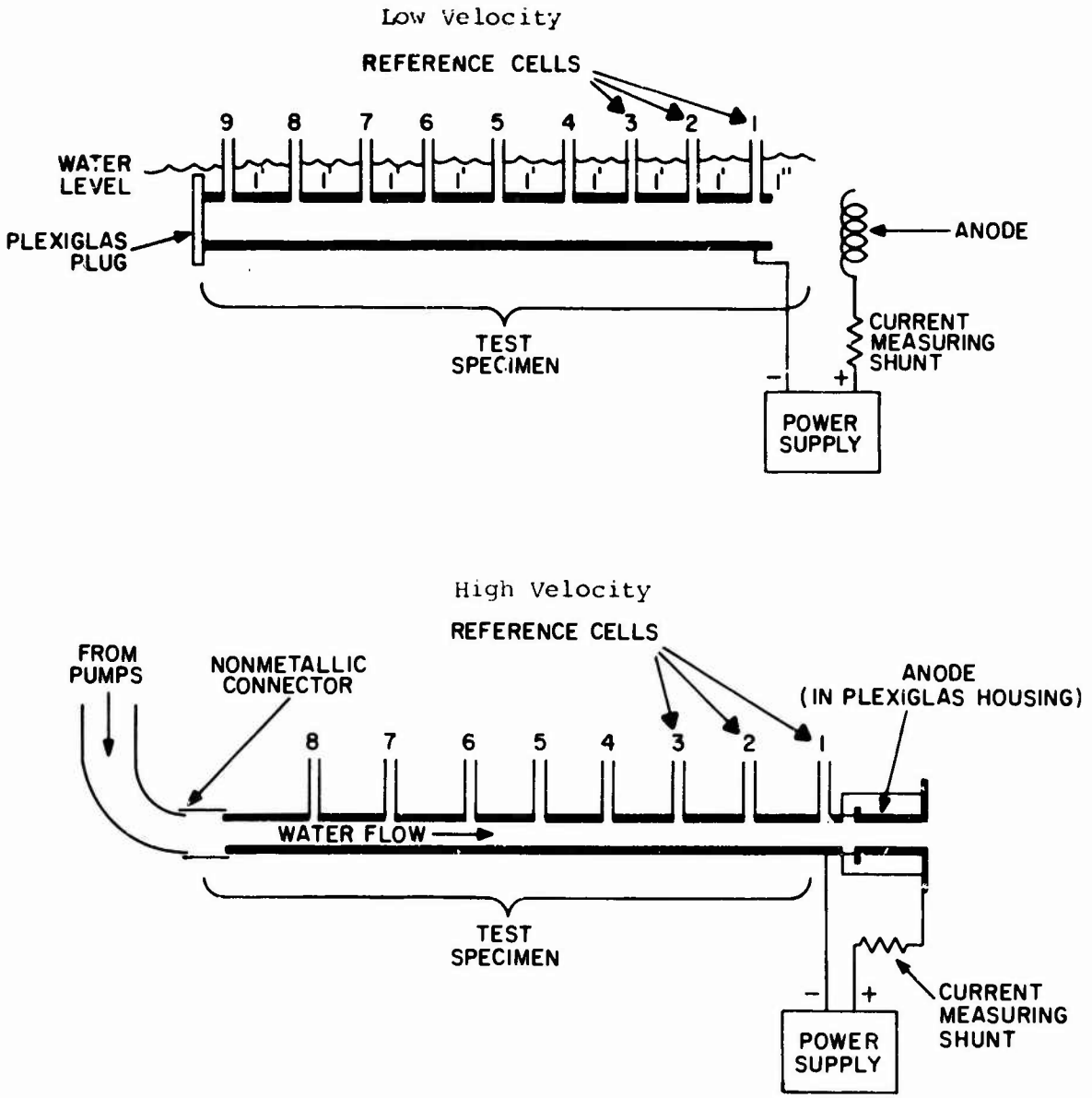

Figure 3
Pipe Test Setup

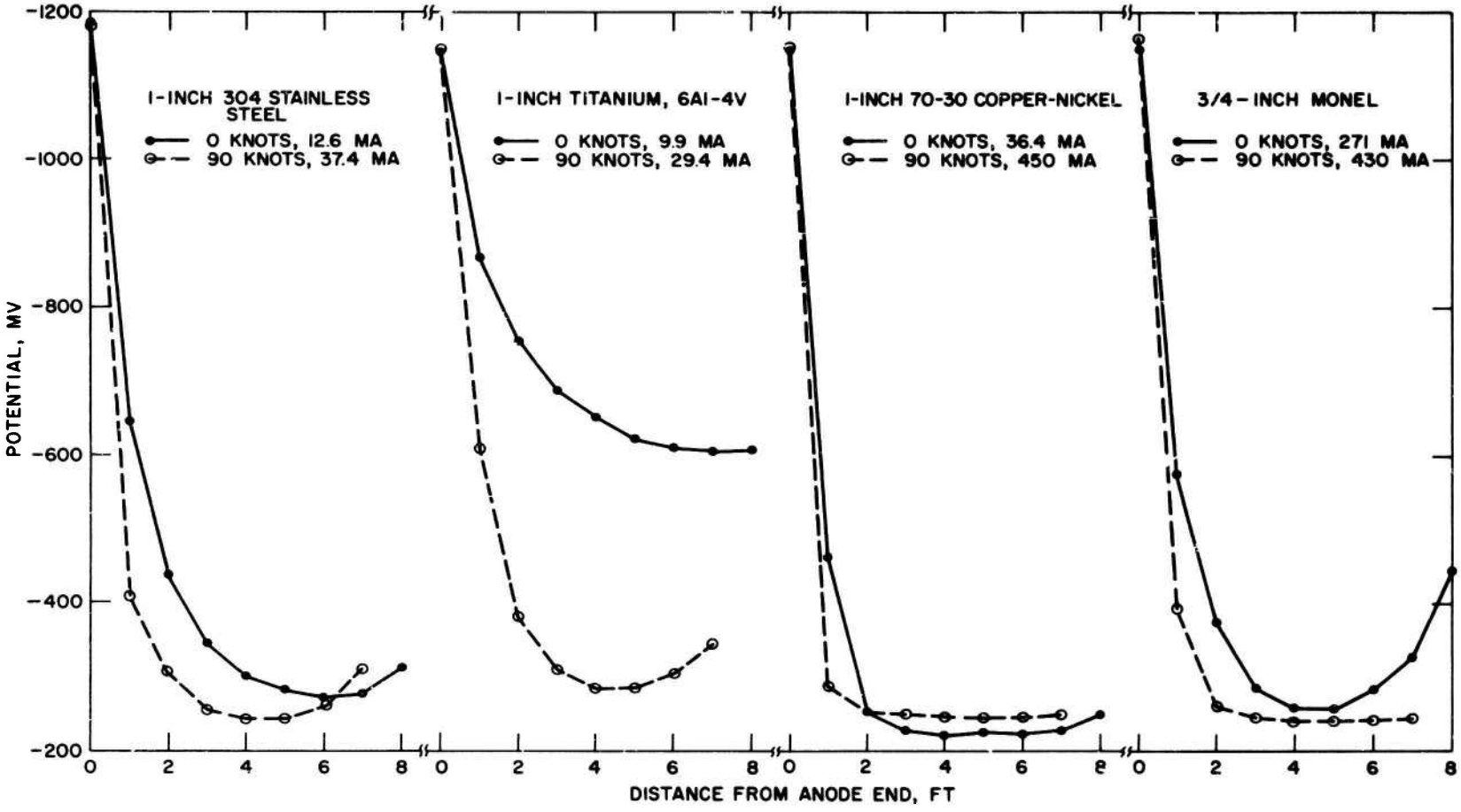

Figure 4
Effect of Velocity on Potential Profiles at -1150 mV

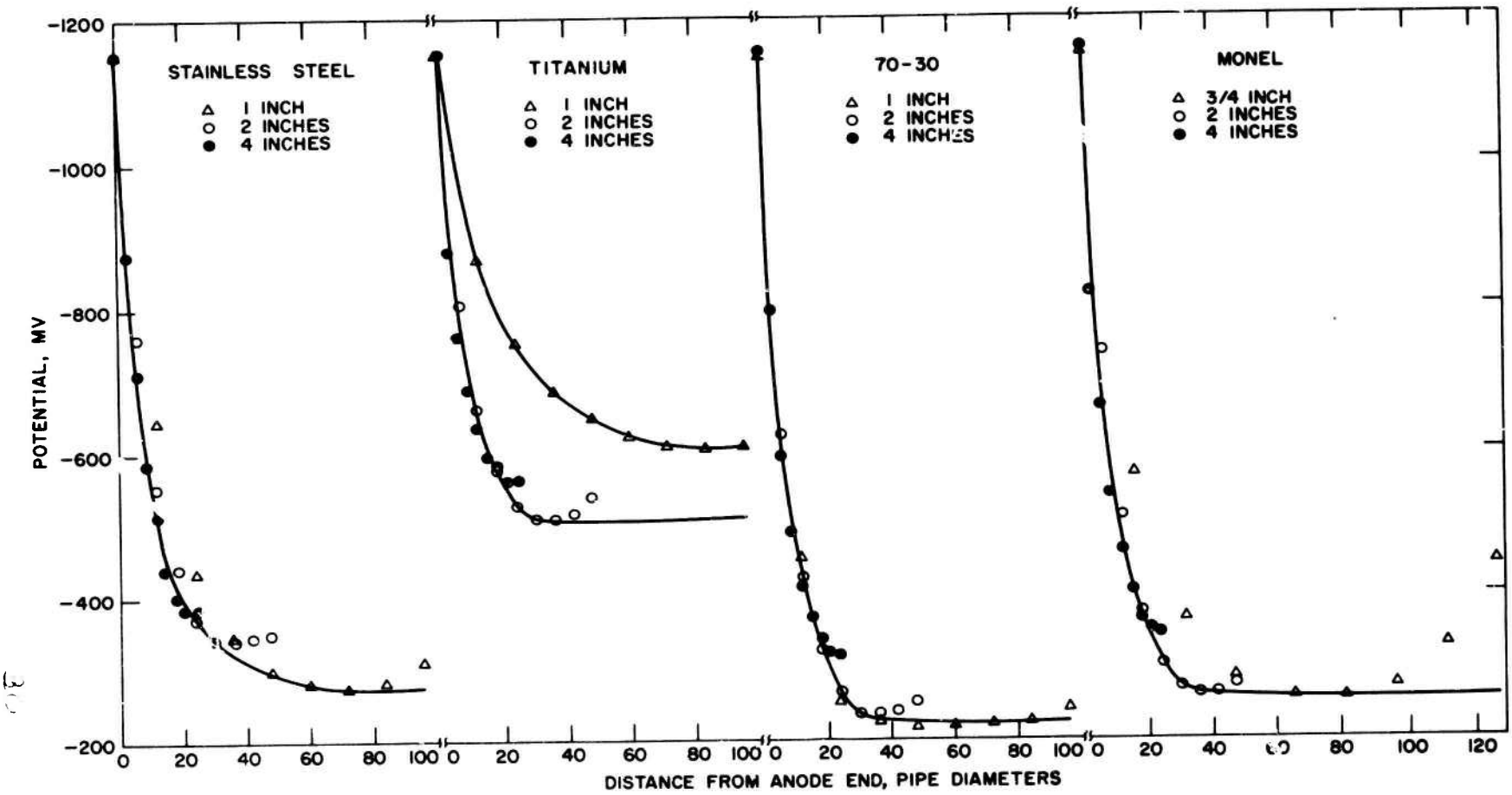

Figure 5
Effect of Internal Diameter on Potential Profiles at 0 Knot and -1150 mV

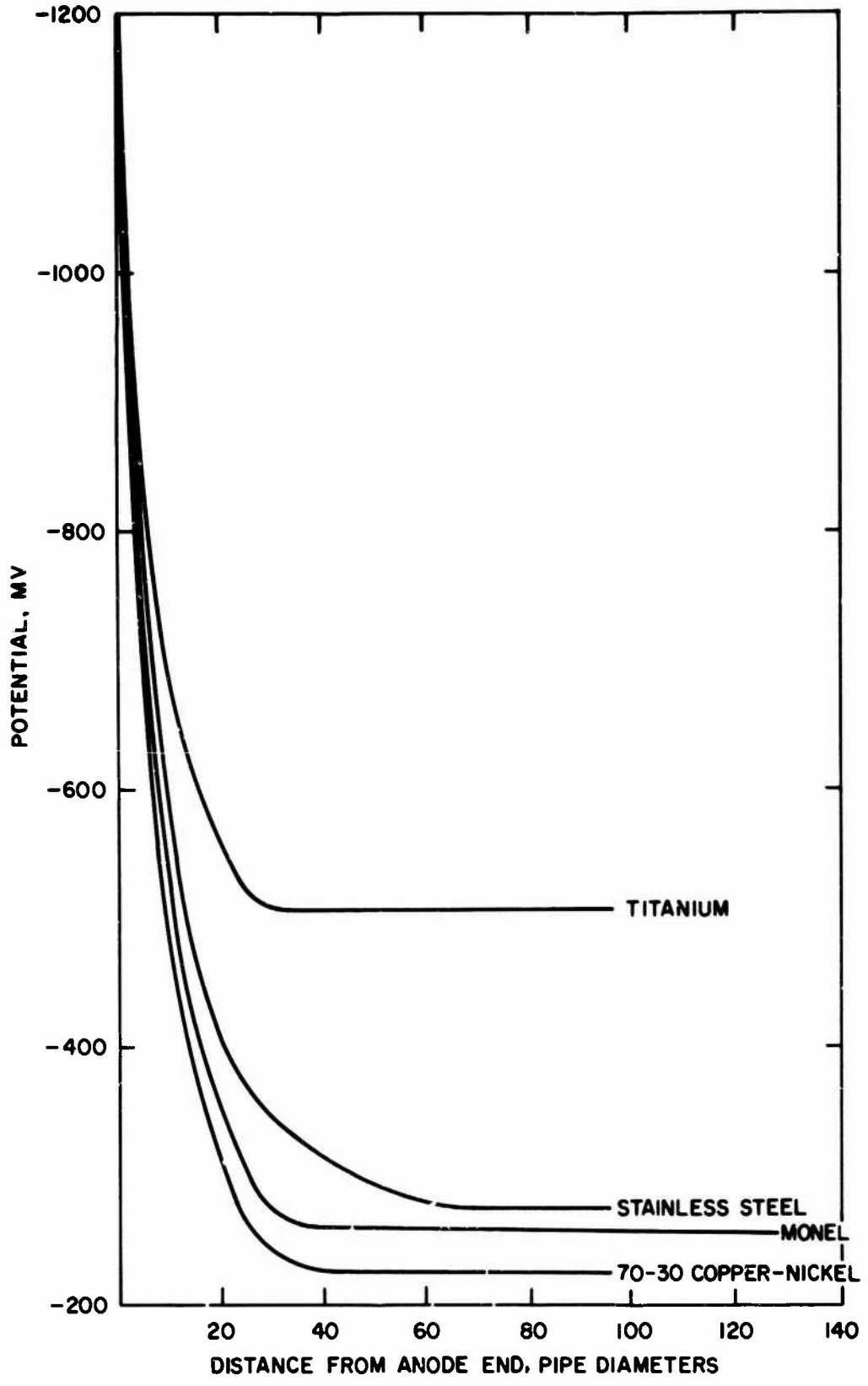

Figure 6
Effect of Material on Potential Profiles
at 0 Knot and -1150 mV

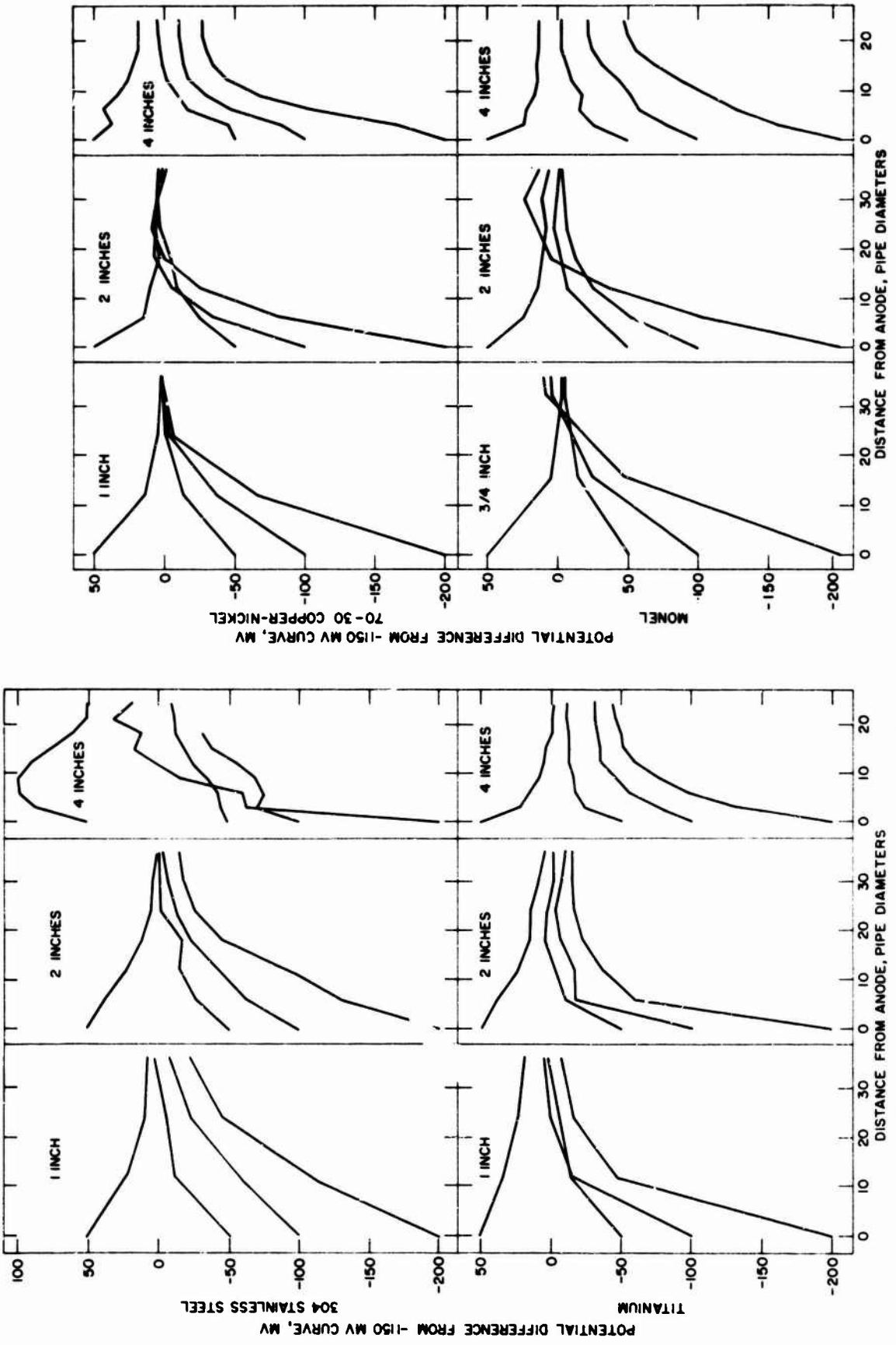

Figure 7 - Effect of Deviation of Protection Potential from -1150 mV on Potential Profiles

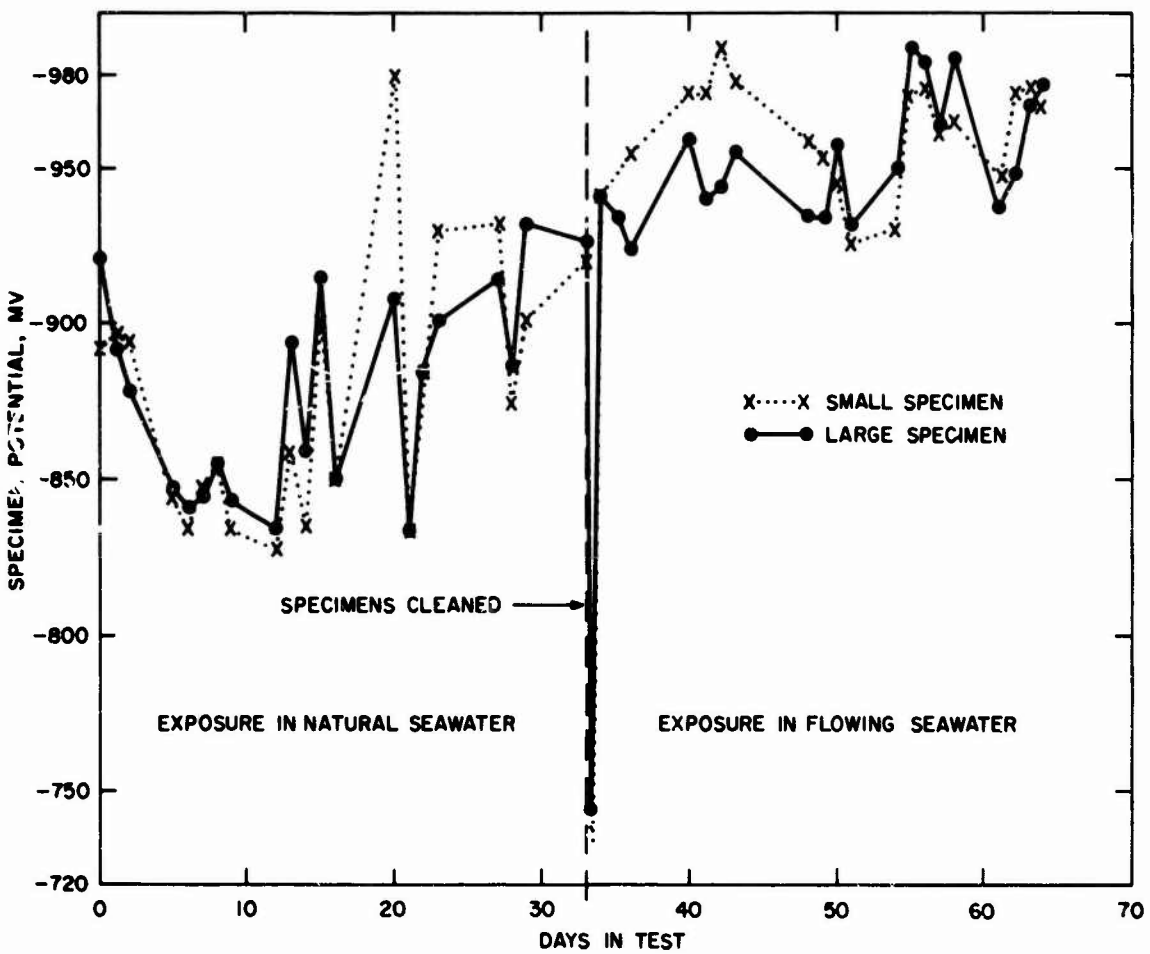

Figure 8
Open-Circuit Potentials of Large and Small Aluminum Specimens

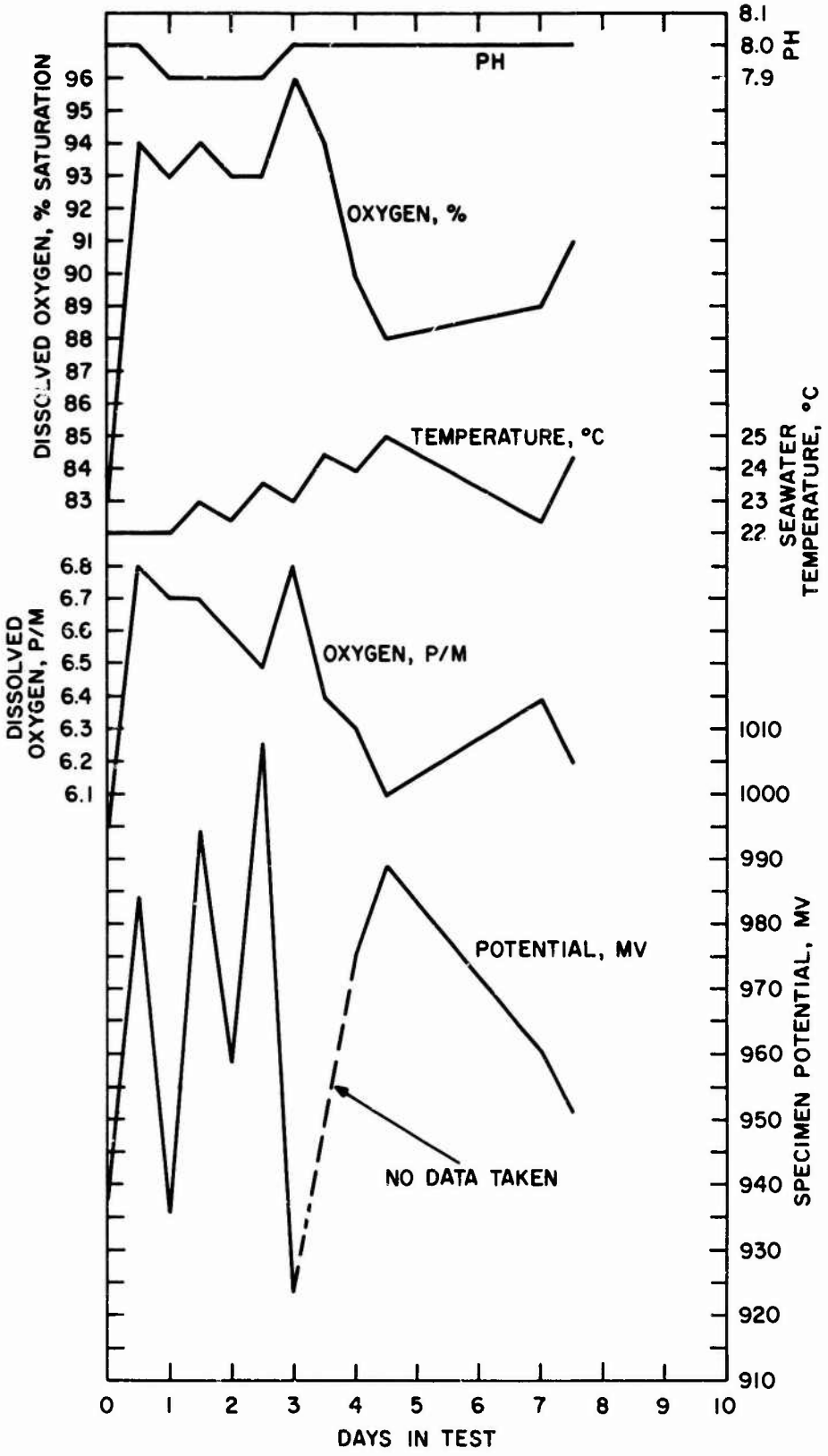

Figure 9
Effect of Seawater Variables
on the Potential of Aluminum

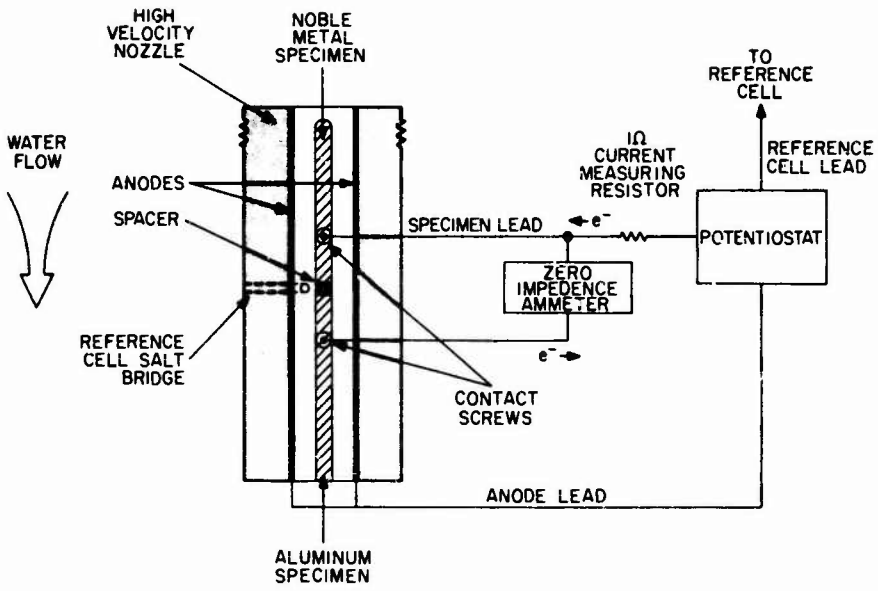

Note: Direction of positive current flow is indicated by: e^- →

Figure 10
High Velocity Galvanic Couple Experimental Setup

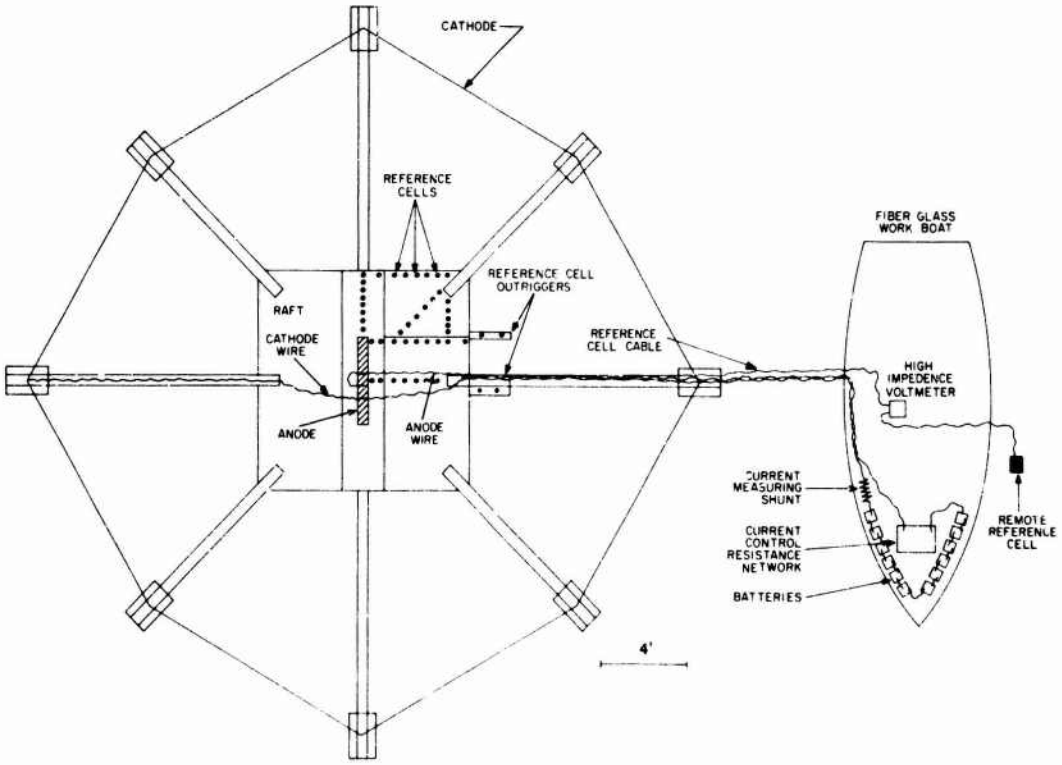

Figure 11
First Raft

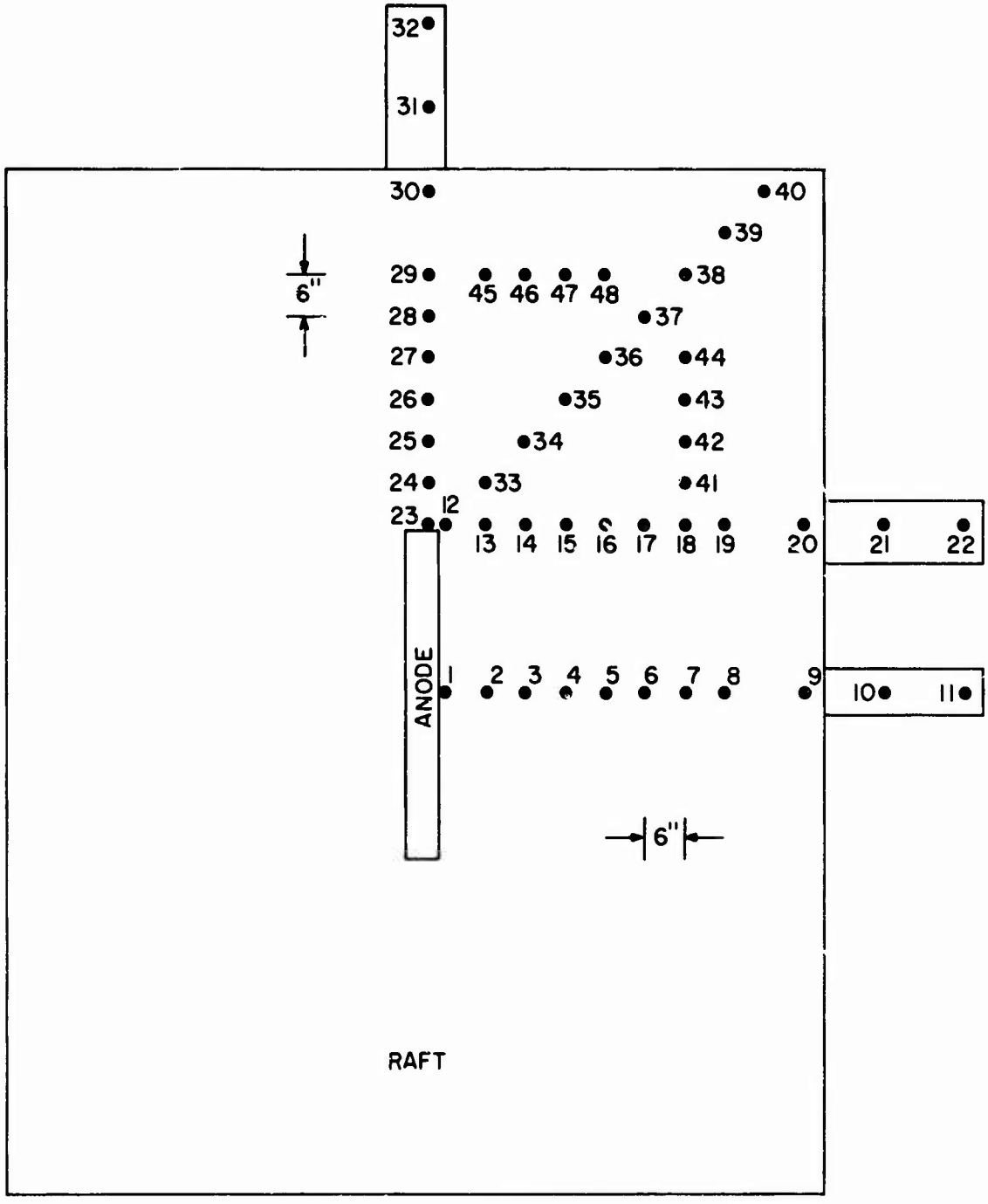

SCALE: 1"=2'

Figure 12
Location of Reference Cells in First Raft

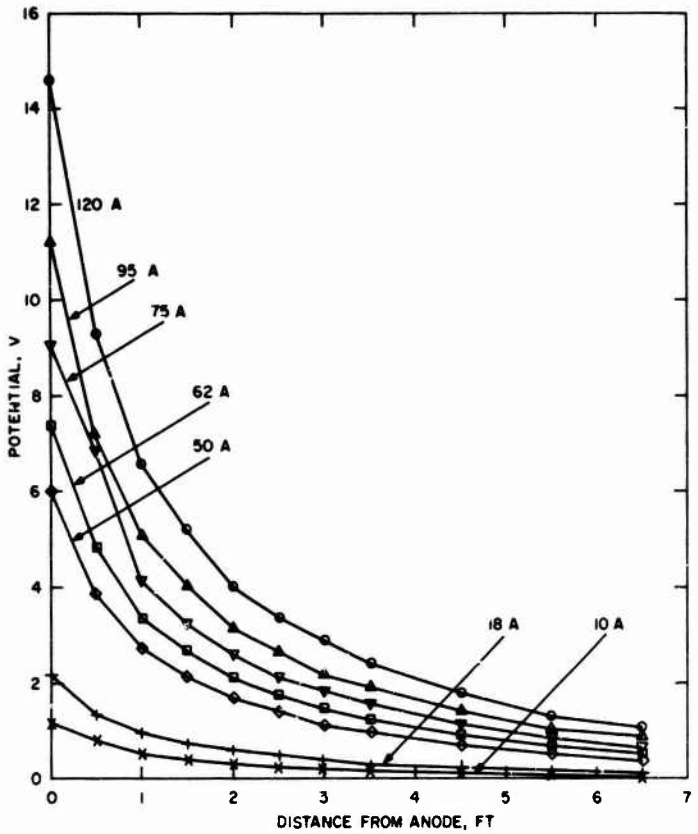

Figure 13
Maximum Potential
(Mid Anode, Cells 1-11)

Figure 14
Minimum Potential
(Side of End Anode,
Cells 12-22)

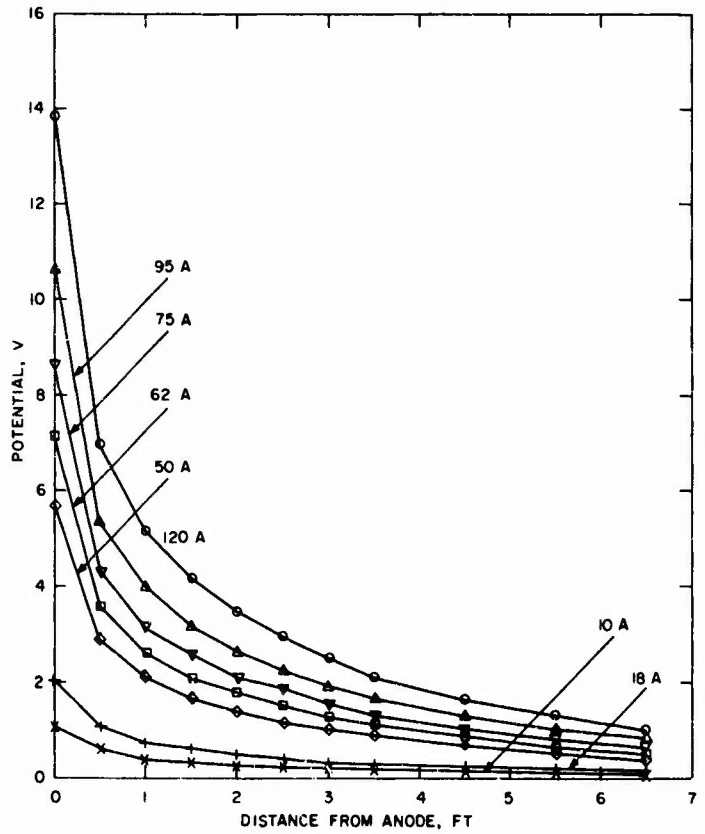

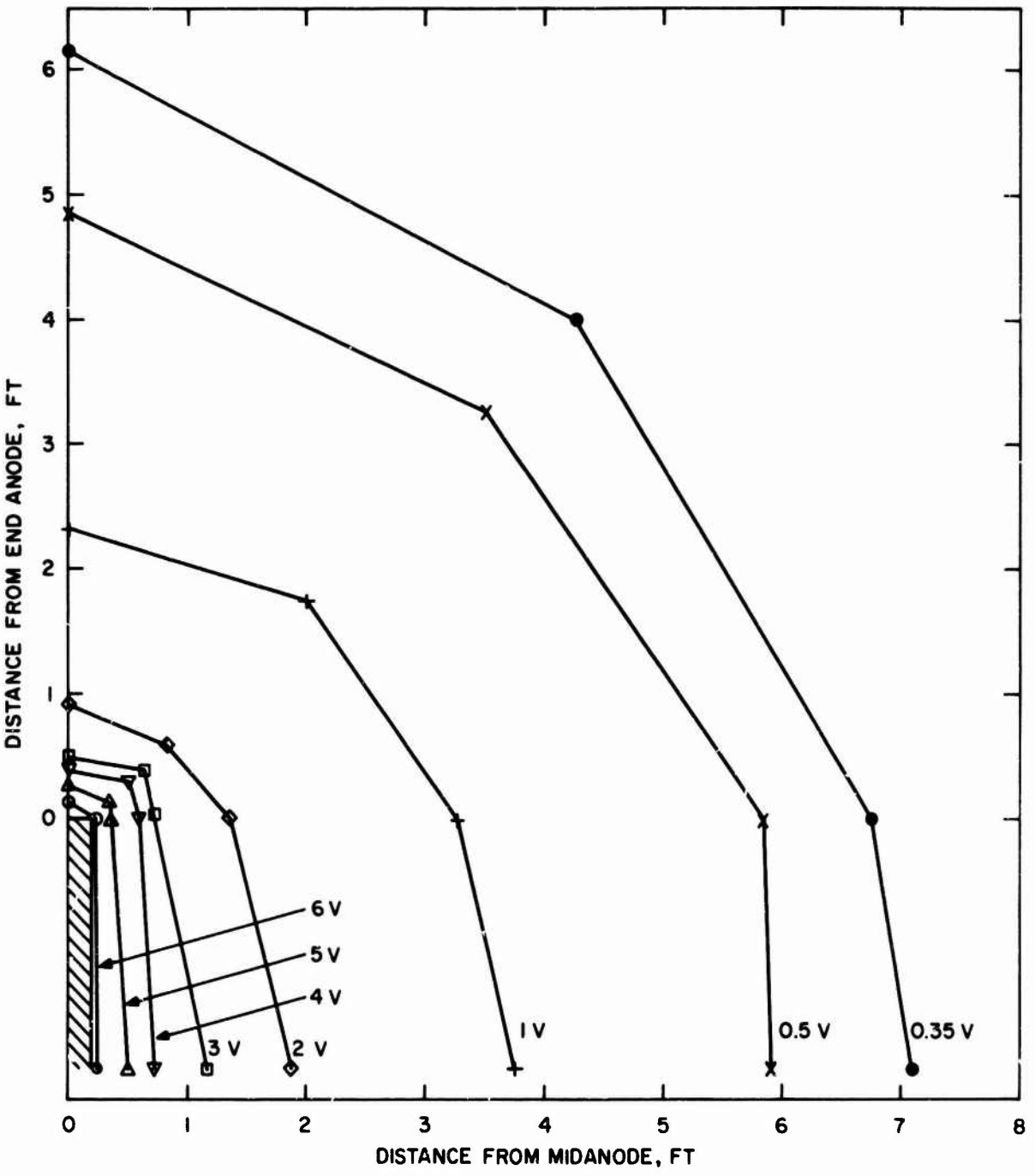

Figure 15
Equipotential Representation, 50 Amperes

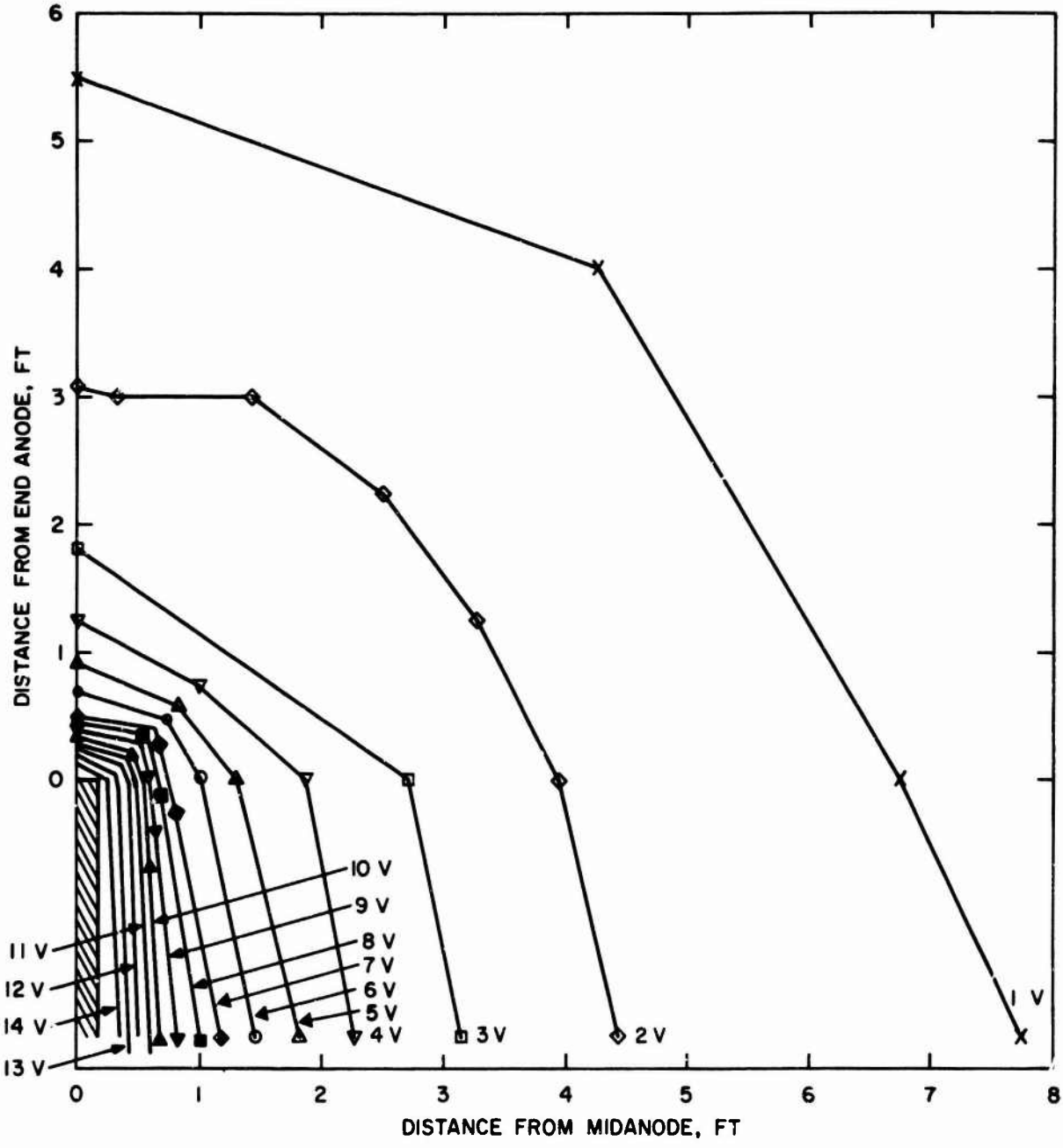

Figure 16
Equipotential Representation, 120 Amperes

4531

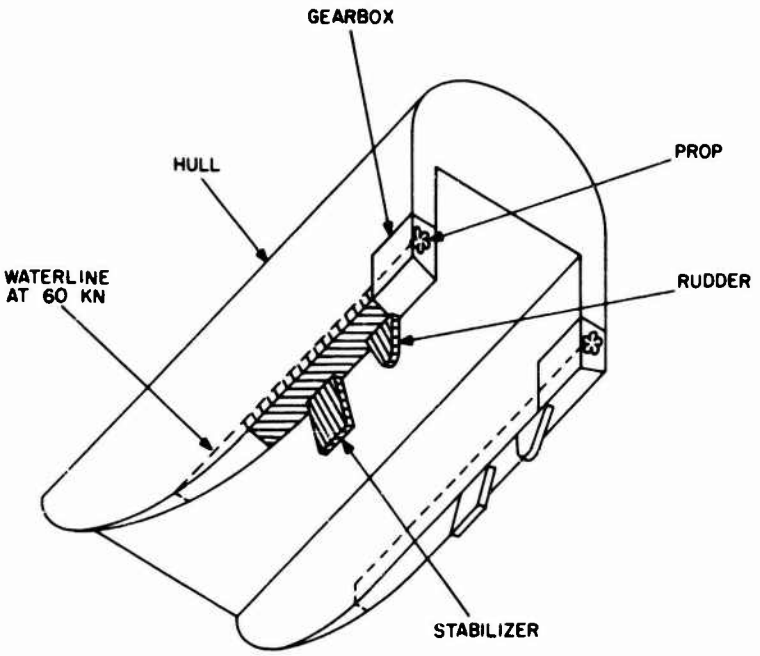

NOTE:
SHADED AREA IS THE SECTION
SIMULATED BY THE TEST RAFT.

Figure 17
Section of Surface Effect Ship Simulated
by Second Raft

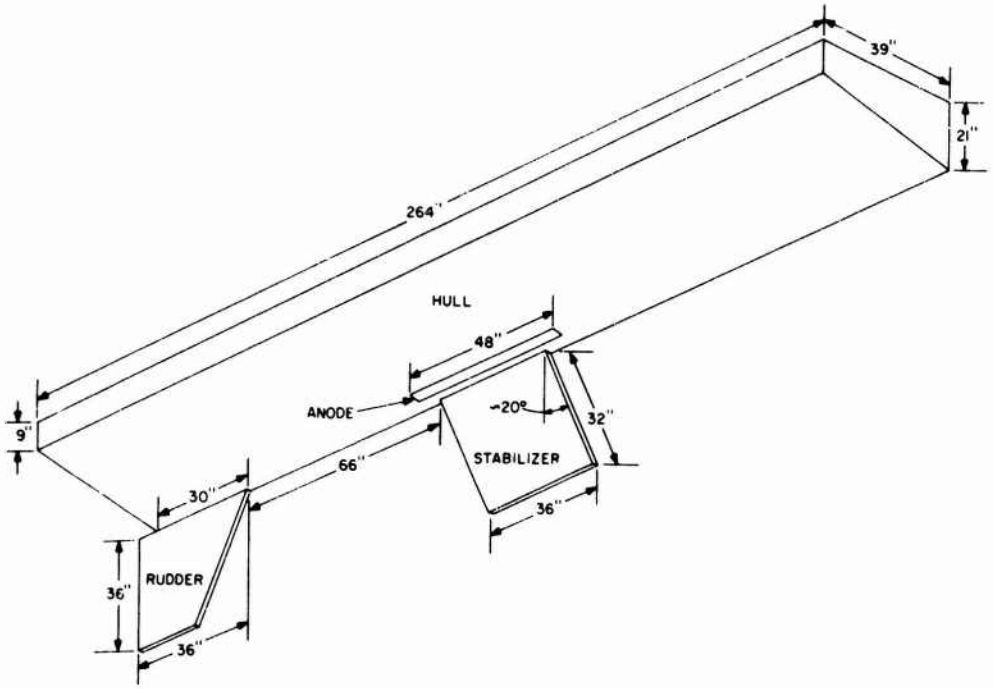

Figure 18 - Second Raft Section

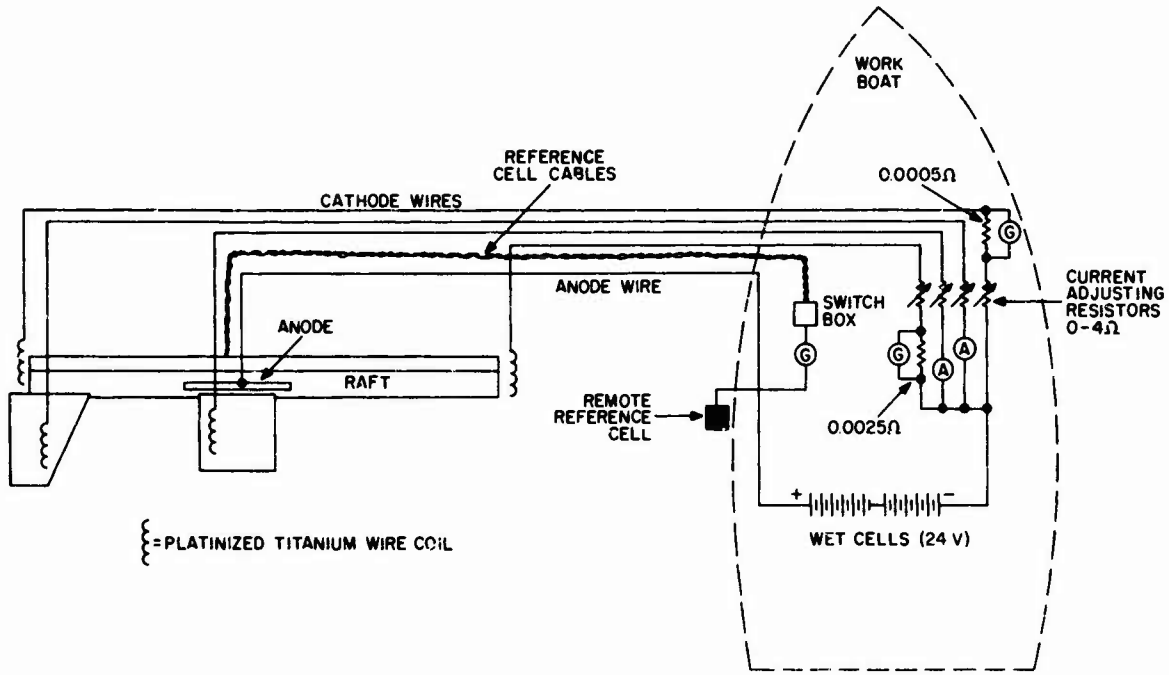

Figure 19
Wiring Diagram of Second Raft

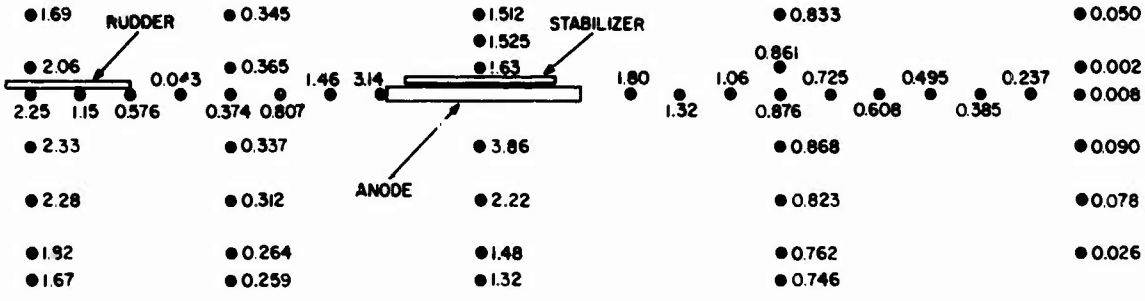

Location	Part	Material	Area Each Side 15-Inch Keel Depth ft²	Effective Area After Coating 1.5% Defects ft²	Maximum Current Density @ Knots ampere/ft²	Maximum Current amperes	Scale Current 1.2 amperes	Actual Current amperes
Near end	Propeller blades	Ti	16.5	8.3 (50% isolated, uncoated	4.85	40.2	-	-
	Propeller hub	SS	6.1	3.1 (50% isolated, uncoated	5.73	17.5	-	-
	Propeller fairwater	SS	3.6	1.8 (50% isolated, uncoated	5.73	10.3	-	-
	Gearbox	SS	24.0	2.5	5.73	14.3	-	-
Total						82.1	98.5	98.
Far end	Hull	Al	2[illegible]	2[illegible]	1.13	24.[illegible]	12.[illegible]	1.[illegible]
Stabilizer	Stabilizer	Ti	15.	1.5	4.85	6.7	4.3	4.7
Rudder	Rudder	Ti	13.5	1.4	4.85	6.8	3.4	3.6

Figure 20
Potentials with Propeller 50% Isolated

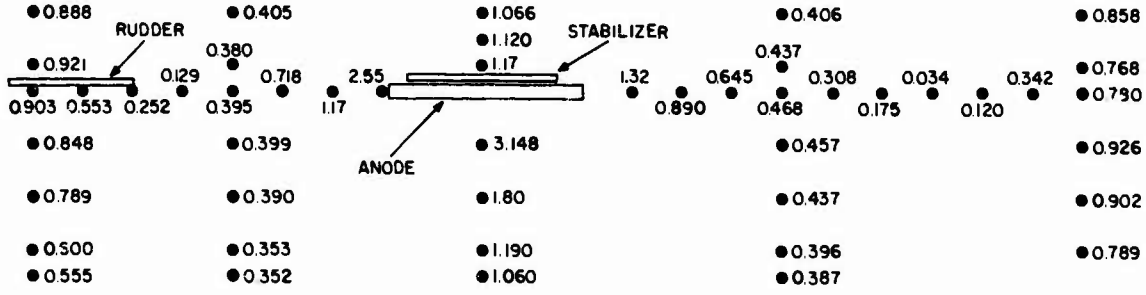

Location	Part	Material	Area Each Side 15-Inch Keel Depth ft²	Effective Area After Coating 1.5% Defects ft²	Maximum Current Density @ Knots ft²	Maximum Current amperes	Actual Current amperes
Near end	Gearbox	SS	24.0	2.5	5.73	14.3	14.3
Far end	Hull	Al	2[illegible]	2[illegible]	1.13	24.[illegible]	1.[illegible]
Stabilizer	Stabilizer	Ti	15.	1.5	4.85	6.7	6.7
Rudder	Rudder	Ti	13.5	1.4	4.85	6.8	6.8

Figure 21
Potentials with Propeller Fully Loaded

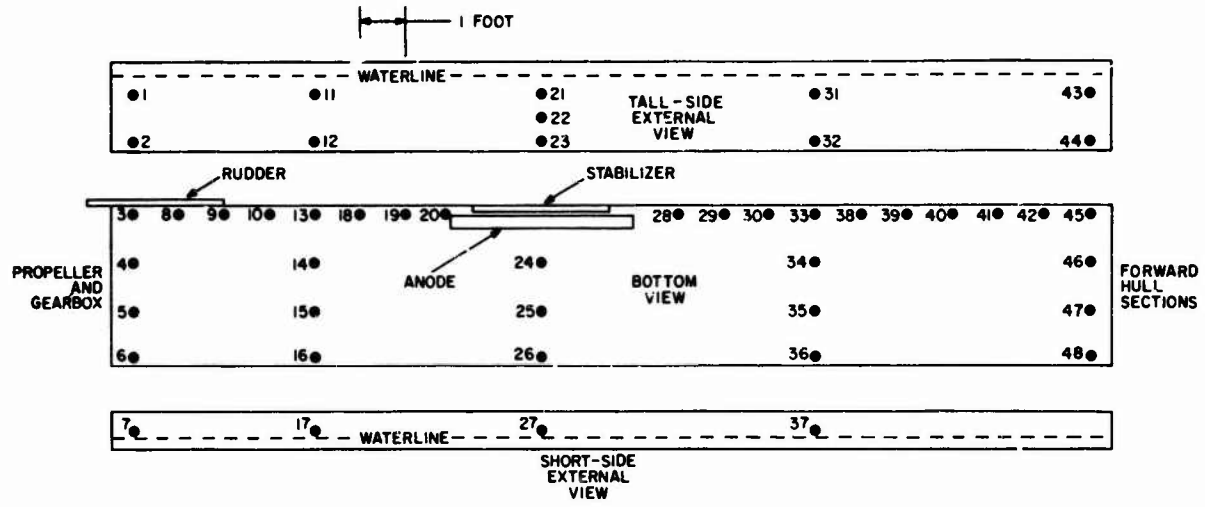

Figure 22
Location of Reference Cells in Second Raft

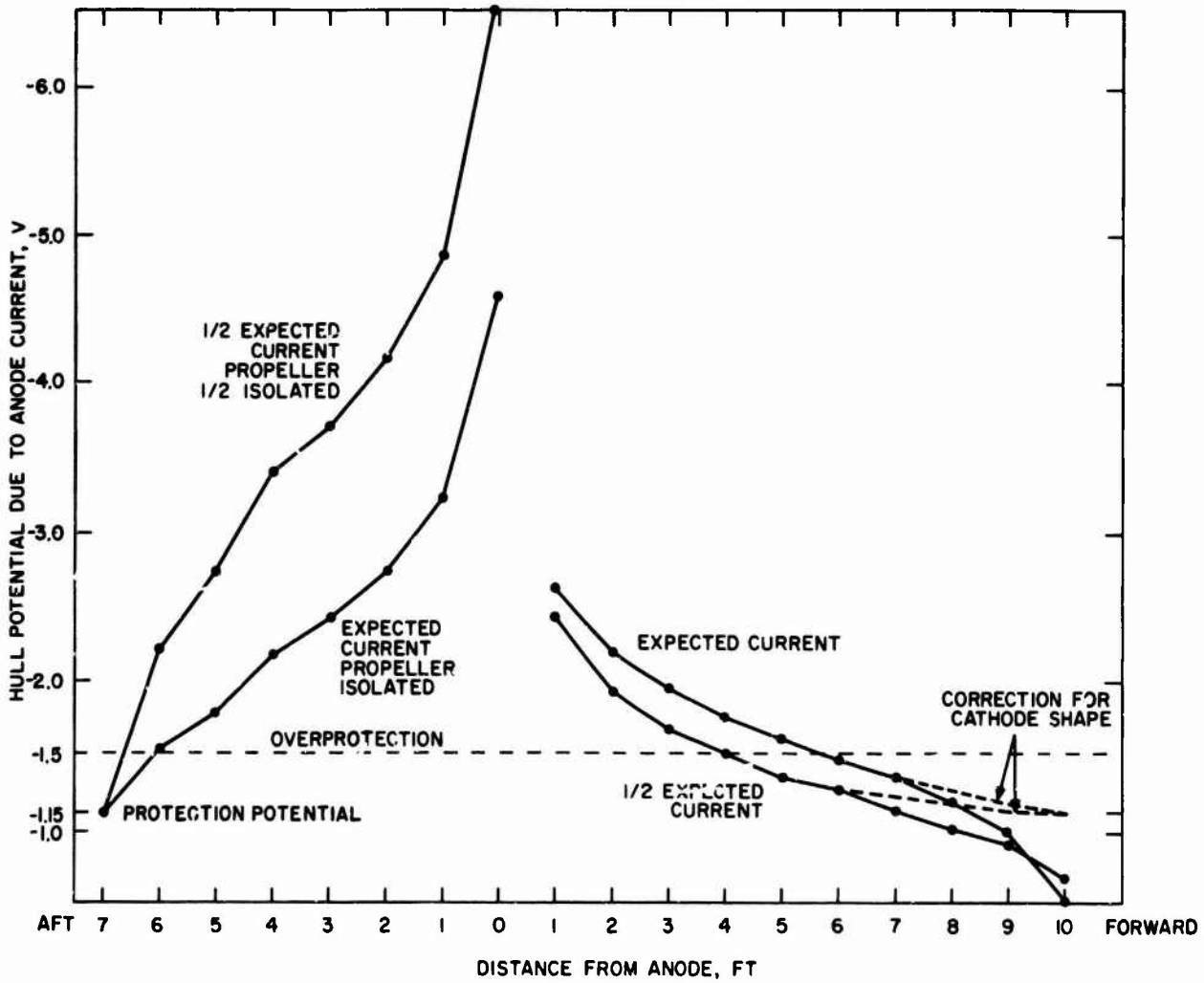

Figure 23
Longitudinal Potential Profiles

4531

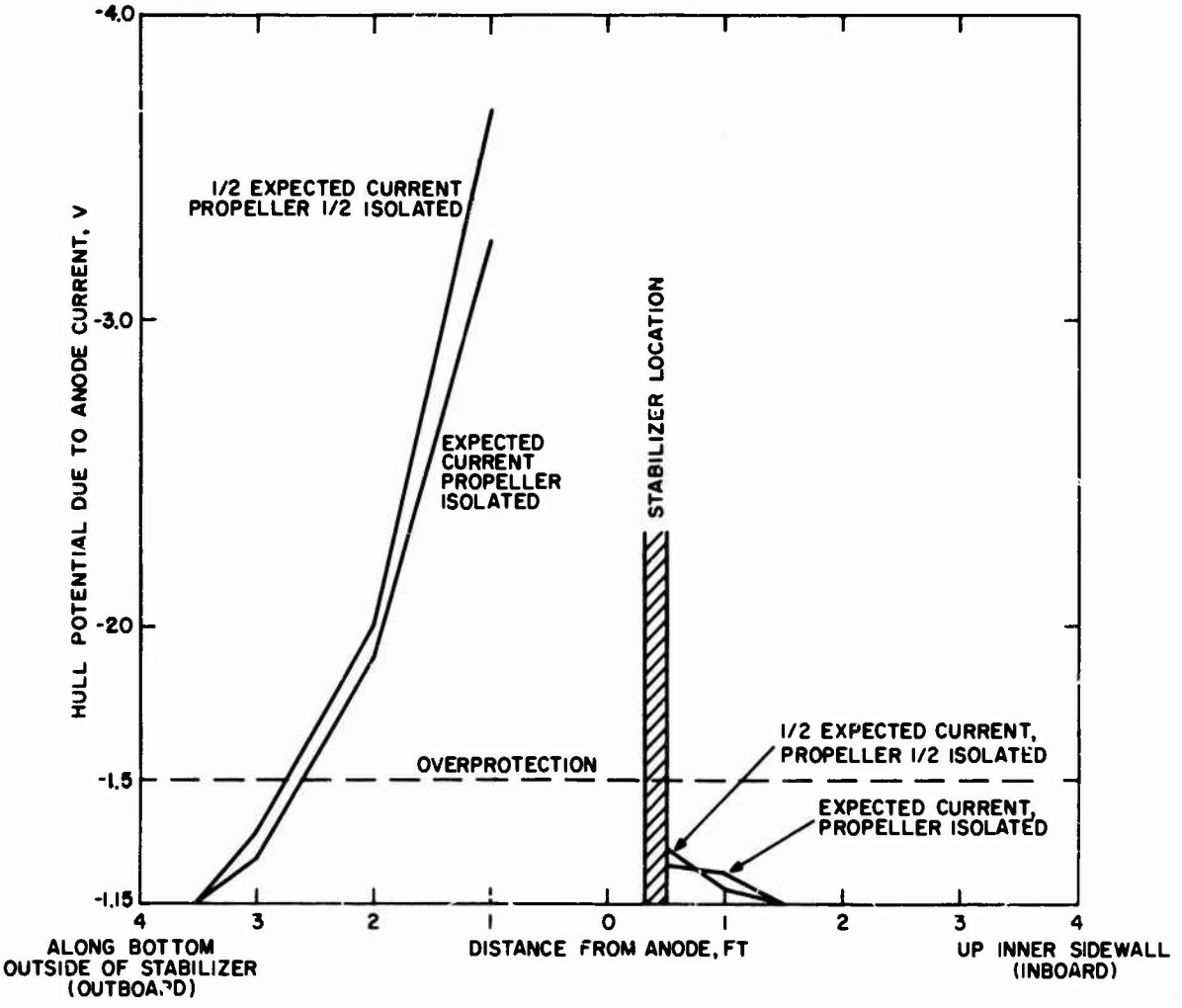

Figure 24
Thwartships Potential Profiles